THE ASTROPHYSICAL JOURNAL, 407:489–509, 1993 April 20

WHAT DETERMINES THE MORPHOLOGICAL FRACTIONS IN CLUSTERS OF GALAXIES?

BRADLEY C. WHITMORE AND DIANE M. GILMORE
Space Telescope Science Institute, 3700 San Martin Drive, Baltimore, MD 21218

AND

CHRISTINE JONES
Smithsonian Astrophysical Observatory, Harvard-Smithsonian Center for Astrophysics, 60 Garden Street, Cambridge, MA 02138
Received 1992 May 8; accepted 1992 October 16

ABSTRACT

A reexamination of Dressler's sample of nearly 6000 galaxies in 55 clusters shows that the morphology-clustercentric radius relation is more fundamental than the morphology–local density relation. This conclusion is supported by improved correlations when the clustercentric radius is used as the independent parameter, and by a comparison of galaxies with the same normalized clustercentric radii but different values of the local density. The morphology-radius relation, when normalized by a characteristic cluster radius, R_c^{opt}, does not vary as a function of the number density within 0.5 Mpc, $N_{0.5}$, the X-ray luminosity, L_X, or the velocity dispersion of the cluster, V_{disp}. This surprising result means that only one parameter is needed to determine the morphological fractions in clusters, namely R/R_c^{opt}. The elliptical fraction in the outer regions of clusters is relatively constant for all types of clusters, with a slight rise from about 10% in the outermost region to about 16% at $R/R_c^{opt} = 1$. For radii smaller than $R/R_c^{opt} = 1$ (generally about 0.5 Mpc for most clusters) the elliptical fraction rises rapidly, reaching values of 60%–70% near the center of the cluster. The S0 fraction rises moderately as the center is approached, and then falls sharply within about 0.2 Mpc of the center. The spiral fraction falls moderately as the clustercentric radius decreases and then falls rapidly near the center. The spiral fraction is essentially zero at the cluster center, even though spirals dominate everywhere else in the universe.

These results indicate that some property of the cluster center plays the key role in determining the morphological fractions in clusters, and suggests the possibility that a destructive mechanism is controlling the morphological fractions rather than a formation mechanism. Using this basic idea as a starting point we developed the following simple model. The three basic assumptions are (1) the intrinsic morphological mix of galaxies is E/(S0 + S + I) = 10%/90%, (2) elliptical galaxies form first, followed by the cluster collapse, S0 galaxies, and finally spiral and irregular galaxies, and (3) during the cluster collapse, galaxies which are still protogalactic clouds of gas are destroyed, and the gas from these failed galaxies is added to the intracluster medium. The destruction of the late-forming spiral and S0 protogalaxies near the cluster centers results in the increase in the elliptical fraction. This simple model can explain a wide range of observations. Besides explaining the morphological fractions, it also suggests that roughly half of the intracluster gas resulted from "failed" galaxies. The model is also consistent with the tidal radii that would be imposed by the mean tidal field of the clusters.

Subject headings: galaxies: clustering — galaxies: fundamental parameters

1. INTRODUCTION

One of the most basic characteristics of a galaxy is its morphological type, and yet we still do not know what causes this diversity. An important clue should be the fact that elliptical galaxies are more prevalent in the centers of clusters, while spiral galaxies dominate in the outer regions of clusters and in the field (Hubble & Humason 1931; Oemler 1974; Melnick & Sargent 1977). However, Dressler's (1980) discovery of a relationship between morphological fraction and local projected galaxy density has focused most recent work on the existence of substructure in clusters (e.g., Fitchett 1988), rather than the question of what determines the morphology of galaxies. While substructure undoubtedly exists in many clusters, a recent study by Sanromà & Salvador-Solé (1990) shows that it cannot be the primary determinant of the morphological fractions in clusters, since a random scrambling of the galaxies along annuli at the same distance from the cluster center (i.e., the destruction of any substructures that might exist) does not change the observed morphology-density relation. Our goal in this paper is to reexamine the question of what does control the morphological fractions in clusters of galaxies.

The theories for the origin of morphological segregation in clusters can be divided into three basic classes. We can fix the morphological types at birth (initial conditions); we can start with all of one type of galaxy and let them evolve toward other types depending on their environment (late evolution; e.g., disks evolve toward S0s via ram-pressure stripping and/or toward ellipticals via mergers); or we can start with a certain mix of morphological types and let them evolve depending on their environment (hybrid models). The situation is reminiscent of the basic psychological question of whether "nature or nurture" (or equivalently, whether "heredity or environment") determines the personality of human beings. For the psychological question, at least, the answer appears to be that a hybrid model is required. We will argue that a hybrid model is also the correct answer in the astronomical case.

How are we to determine which of these theories are most relevant? The approach taken in this paper will be to deter-

mine which parameters result in the best correlations with the morphological fractions in clusters. Dressler (1984) and Whitmore (1990) review a wide range of both local mechanisms (e.g., mergers) and global mechanisms (e.g., tidal shear from the mean cluster field). Each of these different mechanisms would result in a different set of correlations with various physical parameters (e.g., vs. local galaxy density, clustercentric positions, X-ray flux, cluster concentration, velocity dispersion, etc.). This should allow us, at least in principle, to determine which are the relevent physical mechanisms.

In an earlier paper (Whitmore & Gilmore 1991, hereafter WG) we showed that, contrary to earlier findings, the correlation between morphology and projected clustercentric radius is as good, or slightly better, than the correlation between morphology and local projected galaxy density. We found that the fraction of galaxies that were ellipticals was nearly constant throughout most of the cluster, and only within the inner 0.5 Mpc does the fraction of ellipticals rise dramatically. For clusters with D galaxies, the fraction of ellipticals near the centers of the clusters is about 60%. We also found that within 0.2 Mpc of the cluster centers the fraction of S0 galaxies falls rapidly.

In the current paper we continue with this line of attack using new information about the X-ray properties of the clusters, the contamination by background and foreground galaxies, and the effect of various selection biases (e.g., the cutoff at 16th magnitude). Section 2 describes how some of this new information is used to "tune up" the morphology-clustercentric radius relation. In § 3 we examine correlations between morphological fractions and various observational parameters (i.e., central number density, velocity dispersion, and X-ray luminosity) and revisit the question of which is more fundamental, the relation between morphological fraction and projected clustercentric radius, or the relation between morphological fraction and projected local galaxy density. In § 4 we present a simple model which explains several of the correlations and suggests that roughly half of the X-ray gas in clusters came from failed spiral and S0 galaxies. A discussion is provided in § 5.

2. TUNING UP THE MORPHOLOGY-RADIUS RELATION

2.1. *Correction for Foreground and Background Galaxies*

The primary data base used in this study is Dressler's (1980) extensive observations of nearly 6000 galaxies in 55 clusters. The measurement of redshifts for 1267 galaxies in 14 of these clusters by Dressler & Shectman (1988) allows us to tune up the determination of morphological fractions by making more accurate corrections for contamination by foreground and background galaxies. This will be particularly important in determining the exact fraction of ellipticals in the outer regions of clusters.

The first step is to define the velocity range used to determine membership for each cluster. Our assumed values are presented in Table 1, along with the number of galaxies with measured velocities, the number of foreground/background galaxies in each cluster, and the number of foreground/background galaxies which appear to be in groups or clusters of their own (arbitrarily defined as five or more galaxies with velocities within a range of 1000 km s^{-1}). The fraction of superposed galaxies is 156/1267 = 12.3%, corresponding to an average value of 8.8 galaxies per square degree. This is only slightly higher than the value adopted by Dressler (1980) of eight galaxies per square degree. The velocity ranges used to define cluster membership were subjectively determined and are slightly less restrictive than the values Dressler & Shectman used. Using their velocity ranges would add 12 more foreground/background galaxies, and result in a value of 9.5 galaxies per square degree. The difference between these two values represents a fraction of a percent in corrected morphological fractions.

TABLE 1

FOREGROUND/BACKGROUND GALAXIES FOR 14 CLUSTERS

Cluster	V_{min}	V_{max}	Number Measured	Superpositions	Number in Groups
Abell 548	10000	15000	134	1 (1%)	0
Abell 754	14000	19000	89	7 (8%)	0
Abell 1631	12000	16000	90	19 (21%)	17
Abell 1644	11000	17000	103	11 (11%)	6
Abell 1656	3000	9000	102	0 (0%)	0
Abell 1736	9000	16000	104	7 (7%)	0
Abell 1983	10000	16000	100	19 (19%)	12
Abell 2151	9000	14000	105	3 (3%)	0
DC 0003−50 ...	9000	13000	55	19 (35%)	15
DC 0247−31 ...	5000	9000	30	2 (7%)	0
DC 0428−53 ...	10000	14000	100	15 (15%)	7
DC 0559−40 ...	11000	17000	84	7 (8%)	5
DC 0608−33 ...	10000	13000	65	32 (49%)	21
DC 2048−52 ...	11000	16000	106	14 (13%)	0
Totals			1267	156 (12.3%)	83 (6.6%)

NOTES.—Groups are defined as having at least five members within a range of 1000 km s^{-1}.

Of the 156 superposed galaxies, the breakdown by morphological type is E/S0/(S + I) = 42/43/71. A correction is required since there was a bias toward measuring early-type galaxies in the redshift survey. The fractions of galaxies with measured redshifts are E/S0/(S + I) = 327/566/367 = 26.0%/44.9%/29.1%, while the fractions for the galaxies which have been cataloged in all 55 clusters are E/S0/(S + I) = 18.3%/41.0%/40.7%, so of 1260 galaxies with redshifts and types (i.e., excluding type = *U*, unclassified), one should have measured redshifts for 231 ellipticals (i.e., 0.183 × 1260), 517 S0's, and 513 spiral + irregulars in order to not introduce a selection bias. Of these we should have found E/S0/(S + I) = 29.6/39.2/99.2 = 17.6%/23.3%/59.0% were superpositions (i.e., for the ellipticals the calculation is 42/327 × 0.183 × 1260 = 29.6 galaxies).

We therefore shall adopt the following mix of morphological types for the foreground/background galaxies in what follows: E/S0/(S + I) = 18%/23%/59%. While the elliptical fraction is nearly the same as assumed by Dressler (1980; E/S0/(S + I) = 15%/35%/50%; based on 15 plates at random positions on the sky, but with no redshift measurements available), the S0 and spiral + irregular fractions of the superposed galaxies are considerably different. Fifty-three percent of the superposed galaxies are in the groups/clusters we defined. The fact that the foreground/background galaxies tend to be clustered means that simply subtracting a mean value of 8.8 galaxies per square degree is not adequate. There is a tendency for the superposed galaxies to be found in regions of higher density, as shown by Figure 1. For example, while the number of superposed galaxies predicted for a local projected density of log ρ = 1.3 galaxies Mpc^{-2} is only 3%, based on a random distribution, the observed value is 10%. In some cases the superposition of a background or foreground cluster probably

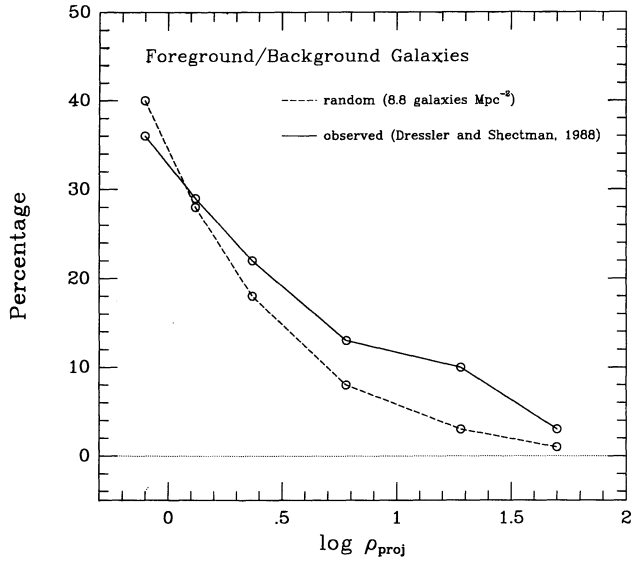

FIG. 1.—Fraction of foreground/background galaxies. Note that in regions of high projected local density the observed contamination fractions are considerably higher than predicted by a uniform distribution. A correction for foreground/background galaxies has been made throughout the paper based on the solid line and the ratios E/S0/(S + I) = 18%/23%/59%, as discussed in the text.

enhanced the apparent density enough to include the cluster in the first place. An example is DC 0608−33, where 49% of the 65 galaxies with measured redshifts are either foreground or background galaxies.

It is important to keep in mind that various correlations that we will be discussing are partially washed out by these superpositions, and by the fact that we must use projected as opposed to true positions in the cluster. The underlying correlations are therefore even stronger than they appear.

Throughout the paper, corrections for foreground/background contamination have been made by using the values of E/S0/(S + I) = 18%/23%/59% and the solid line in Figure 1. For example, at an apparent local density of log $\rho = 0.0$, the contamination fraction is 33%. An apparent elliptical fraction of 12.0% would therefore drop to a corrected value of 9.0% (i.e., $0.33 \times 0.18 + 0.67 \times 0.090 = 0.120$).

Dressler's definition of the local projected galaxy density is used throughout this paper (i.e., the density of galaxies out to a radius defined by the position of the tenth nearest galaxy). We note that although Dressler (1980) corrected his values of the local density for each galaxy, he did not correct the values of the morphological fractions in his diagrams, since the effect is quite small. However, since a determination of the true elliptical fraction in the outer regions of clusters will prove to be quite important for our model, and since the elliptical fraction in the superposed galaxies does turn out to be slightly higher than previously believed, the correction has been made in this paper.

The fact that the elliptical fraction for the foreground/background galaxies is higher than the canonical value of 10% for the field probably indicates that we are picking up some of the brighter elliptical galaxies in the central regions of background clusters. This interpretation is supported by the fact that only 13% of the foreground galaxies are ellipticals, while 33% of the background galaxies and 47% of the background galaxies with recessional velocities over 30,000 km s^{-1} are ellipticals.

2.2. *Correction for Magnitude Cutoff*

Dressler's (1980) sample contains galaxies brighter than an apparent magnitude cutoff of 16.5 in the V-band. This corresponds to a range in the absolute magnitude cutoff from −18.1 for DC 1842−063 at $z = 0.0141$, to −21.4 for Abell 14 at $z = 0.064$. A Hubble constant of $H_0 = 50$ km s^{-1} Mpc^{-1} is used throughout this paper. The cutoff affects the mix of morphological types since the luminosity functions are different for each type. More specifically, the more distant clusters include only the brightest galaxies in the cluster, which tend to be the ellipticals. This results in an artificial enhancement of the elliptical fraction for distant clusters.

The effect of this magnitude cutoff is clearly seen in the data. For example, if we break the sample of 55 clusters into five subsamples in order of redshift, we find that the elliptical fraction in the outer region appears to systematically increase with redshift, from 12% for the nearby sample to 22% for the most distant sample. The comparison is made from 0.5 Mpc to the radius where Dressler's local density parameter falls below a value of 0.5 (i.e., where the contamination from foreground/background galaxies starts to become sizeable).

However, it is possible that some of this correlation with redshift is caused by intrinsic differences between the clusters (e.g., the more distant clusters tend to be stronger X-ray sources and to be richer). We can test this possibility by grouping the clusters into four groups, according to the values of their X-ray luminosity, L_X, and then dividing each group into three redshift subsamples. We assume that the selection of the sample based on X-ray properties groups the clusters into physically similar objects; any differences in the outer elliptical fraction can therefore be attributed to the effect of the magnitude cutoff. We find that the effect persists, with the nearer clusters having outer elliptical fractions which are about 9% lower than the more distant clusters, even though they have the same values of L_X.

A correction for the magnitude cutoff is made using the cumulative luminosity function for each morphological type, as determined by the clusters with redshifts less than $z = 0.035$. This value represents a compromise between using nearby clusters where the luminosity function is sampled to faint magnitude, and the need to keep enough clusters in the sample to provide good statistics. Several clusters (i.e., A496, A1656, A2063, DC 0559−40, DC 0608−33, DC 2345−27) were double-counted in order to correct for the fact that the nearby clusters tend to have lower values of L_X. The resulting sample has roughly the same mix of L_X values as the total sample.

Figure 2 shows the cumulative growth of each morphological type as a function of absolute magnitude. This figure is used to scale the observed galaxy counts to the number of galaxies that would have been observed if an absolute magnitude cutoff of −20.4 had been used (i.e., the cutoff magnitude for a cluster at $z = 0.04$; a typical value for the Dressler clusters). For example, the cutoff for Abell 14 is −21.4, which corresponds to a value of 0.599 for the elliptical line in Figure 2. If the redshift had been 0.04, the cutoff would have been −20.4, and the line in Figure 2 would give a value of 1.00 (i.e., the figure is normalized to have a value of 1.00 for the ellipticals at −20.4). The correction was therefore made by counting each elliptical galaxy in Abell 14 as 1.00/0.599 = 1.669 galaxies. Similarly, each spiral was counted as 1.750/0.838 = 2.088 galaxies. We

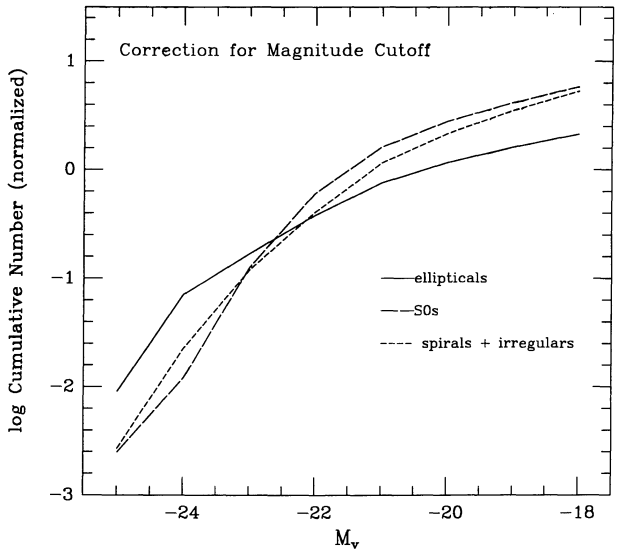

FIG. 2.—Cumulative luminosity function in V for each morphological type as determined from the clusters within $z < 0.035$ (*see text*). This is used to scale the number of galaxies of each type for each cluster to the value the cluster would have if a magnitude cutoff of −20.4 was imposed. The figure is normalized to have a value of 1.0 for the cumulative luminosity function of the ellipticals at a magnitude of −20.4.

note that like the foreground/background correction, Dressler made a correction for the magnitude cutoff in the value of the local projected galaxy density, but not in the determination of morphological fractions which are shown in the figures.

The magnitude cutoff correction removes most of the dependence on z (i.e., the 9%–10% differences reported above are reduced to the level of 2%–3%). The remaining dependence may indicate that the correction is not quite strong enough, it may indicate the presence of some other more subtle bias, or it may represent a real effect of some sort. One other possibility we examined was that spiral galaxies might be preferentially missed at high redshift due to decreasing spatial resolution. This does not appear to be the case, however, since the total number of galaxies in a cluster (after making corrections for different plate size and magnitude cutoffs) does not appear to correlate with redshift.

2.3. *Determination of the Cluster Center*

Beers & Tonry (1986) found that using either the position of the D or cD galaxy in a cluster, or the X-ray center, resulted in the steepest density profile for the cluster. WG therefore used the position of the D galaxy to define the center of the cluster for some aspects of their study. However, this introduced a bias in the determination of the elliptical fraction for the central bin, since by definition an elliptical galaxy was already included. This problem can now be solved by the use of X-ray centers for 39 of the clusters, using data from the compilation of Jones et al. (1993). In a few cases where the X-ray images showed a clearly double-peaked or asymmetric morphology (i.e., A168, A754, A1644, A1913, A2151, DC 329−52, DC 559−40, and DC 622−64), the position of the stronger peak was used to define the cluster center.

Figure 3 shows the morphology-clustercentric radius relation for the 30 clusters with both X-ray centers and D-galaxy centers. We find that the use of D-galaxy centers results in an elliptical fraction of 67% ± 8% for the galaxies within 0.12 Mpc of the center, comparable to the elliptical fraction of 65% ± 8% when X-ray centers are used. Using the galaxy with the highest local density as the center yields only 52% ± 7%. The fact that using X-ray centers results in elliptical fractions which are comparable to the fractions obtained when using D-galaxy centers, even though the results for D-galaxy centers are artificially enhanced by the automatic inclusion of the central elliptical, indicates that the X-ray centers are probably slightly better at defining the center of the cluster. For 10 clusters where X-ray centers have not been determined, the position of the D galaxy will be used as the center in the following analysis. For an additional six clusters where neither an X-ray center or D-galaxy position is available, the position of the galaxy with the highest projected local density is used. The positions of the centers are included in Table 2.

It is possible that the bias introduced by the use of the position of an elliptical galaxy as the center is not completely alleviated by the use of the X-ray centers. For example, if the X-ray center was always aligned with an elliptical galaxy, perhaps due to the enhancement of the elliptical's own X-ray flux on the background of the cluster, a bias would still be introduced. This does not appear to be the case, however, since 67% of the time the nearest galaxy to the X-ray center is an elliptical. This is essentially the same percentage as found in the inner bin.

2.4. *Normalization Using a Characteristic Cluster Radius*

In WG, the projected radius from the center of the cluster is used as the independent variable when comparing morphological fractions. A shortcoming of this technique is that it ignores the fact that at 0.5 Mpc we might be in the outskirts of a small condensed cluster (e.g., DC 0247−31) while 0.5 Mpc is still within the "core" of a large cluster (e.g., the Coma cluster). We have therefore defined a "characteristic radius", $R_c^{\rm opt}$, as the radius at which the *cumulative* projected galaxy density falls below 20 galaxies Mpc^{-2}. The cumulative value is used since the small number of galaxies makes it impossible to determine reasonable values of the actual density at each radii. Values of $R_c^{\rm opt}$ are included in Table 2.

The X-ray data have been used to determine core radii, $R_{\rm core}^{\rm X\text{-}ray}$, for 31 of the clusters (Jones et al. 1993). Some of these clusters are better fitted by a two-component model rather than the one-component model used here. These are indicated in Table 2.

Several other cluster properties also have been computed, or compiled from other sources, and are included in Table 2. These include cluster velocity dispersion, cumulative number of galaxies within radii of 2.0, 1.0, and 0.5 Mpc (after the corrections for superposed galaxies and magnitude cutoff discussed in the previous sections have been made), position used to define the center of the cluster, X-ray luminosity, and the mass of the intracluster gas.

2.5. *Removal of Double Clusters*

Several clusters in the sample have more than one obvious center, which complicates a determination of the morphology-radius relation. In addition, in the case of DC 0326−53 and DC 0329−52, the overlap of about 60 galaxies results in the double counting of these galaxies. We have alleviated these problems in the most obvious cases by removing the galaxies within about 1 Mpc of the secondary cluster center. The clusters affected are: Abell 548 (removed galaxies with $X > 265$ and $Y < 265$), Abell 754 (removed galaxies in the range $240 < X < 300$, $220 < Y < 300$), DC 0326−53 (removed

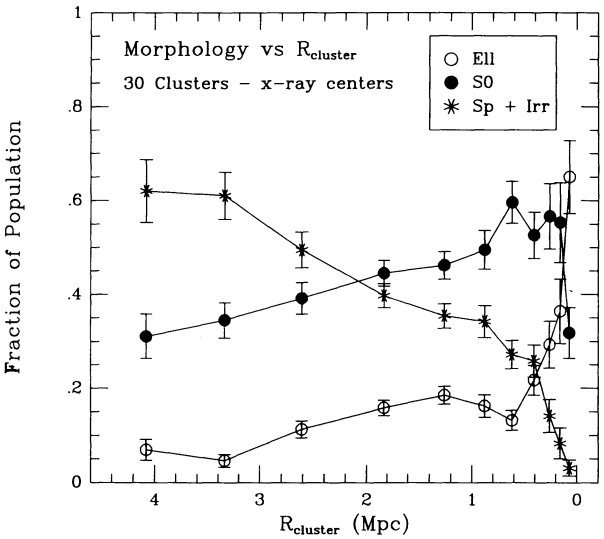

FIG 3*a*

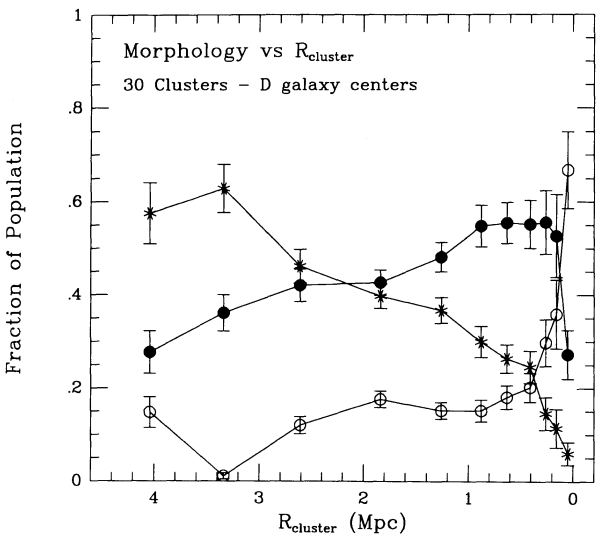

FIG. 3*b*

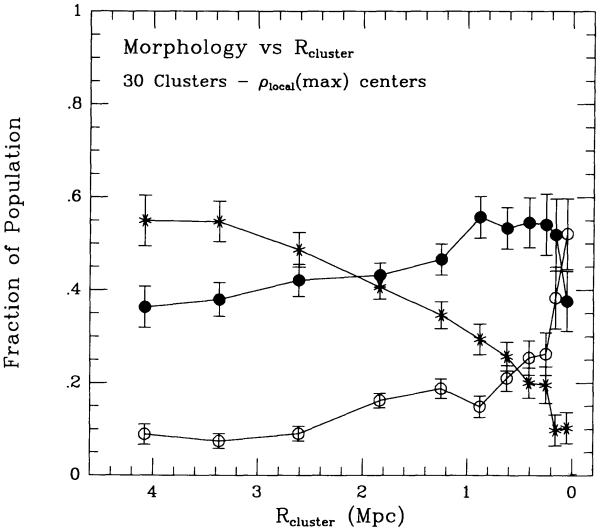

FIG. 3*c*

FIG. 3.—Morphology-clustercentric radius relation for the 30 clusters with both X-ray data and a central D galaxy. Panel *a* shows the result when X-ray centers are used; panel *b* shows the result when D-galaxy centers are used; and panel *c* shows the result when the galaxy with the highest local projected density is used for the center. The key for the different morphological types is included in panel *a* and is used for the subsequent figures.

about 30 galaxies in the NW corner), DC 0329−52 (removed about 30 galaxies in the SE corner), DC 0559−40 (removed galaxies in the range $90 < X < 150$, $370 < Y < 430$, and the range $210 < X < 290$, $210 < Y < 290$). The criteria used to determine these double clusters was that the secondary center must have a D galaxy or a clear concentration of galaxies around it, and must be well separated from the main center. In most cases there was also evidence from the X-ray data for a second component.

The overlap of galaxies in DC 0326−53 and DC 0329−52 (plus two more that overlap in Abell 978 and DC 979) allows us to check on the repeatability of the morphological classifications. In the region of overlap, 56 galaxies are included on both plates, while 15 are included on one plate but not the other (i.e., there are seven on the DC 0329−53 plate which are not on the DC 0326−52 plate, and eight on the DC 0326−52 plate which are not on the DC 0329−53 plate). Of the 56 galaxies in common, 44 have the same classification. Of the 12 galaxies with different classifications, the most common case is a switch between spiral and S0 (8/12 cases). In no case is there a switch between spiral and elliptical classifications.

We also might mention that there are other cases where, although there is no overlap in plate material, one cluster is probably just the outskirts of the other, rather than representing a separate cluster. These are DC 103−47 and DC 107−46 (where the NE corner of DC 103−47 is blanked out by Dressler to remove any overlap), and DC 2345−28 and DC 2349−28. Other cases of clusters that are close together, but are probably distinct, are Abell 978/979/993 and Abell 1983/1991.

3. MORPHOLOGICAL FRACTIONS IN CLUSTERS OF GALAXIES

Figure 4 shows the morphology-clustercentric radius relation for all 55 clusters, after correcting for foreground/background galaxies, the magnitude cutoff, new cluster centers, and the removal of double clusters. We find that the elliptical fraction has increased from 44% ± 5% (Fig. 2 from WG) to 59% ± 6% for galaxies within 0.12 Mpc of the cluster center. The drop in the S0 fraction near the center is also more convincing than in WG. The percentage of spirals in the inner bin is now only 6% ± 2%.

There is a slight gradient of the elliptical fraction in the outer regions of clusters, unlike WG where the elliptical fraction was almost perfectly flat. This results primarily from the new foreground/background correction. Although the gradient is quite small (i.e., an increase from 10% ± 1% at 4 Mpc to 16% ± 1% at 0.6 Mpc), it does represent a factor of 1.6 increase over this range. While the changes in the spiral and S0 fractions over this range are much larger (25%–35% rather than the 6% for the ellipticals), in relative terms they are only slightly larger (i.e., a factor of 2.0 instead of 1.6). This weakens the conclusion by WG that the spirals and S0s are controlled by a different mechanism than the ellipticals. While the complementary nature of the gradients still suggest a link between spirals and S0s (e.g., conversion of spirals to S0s via ram-

TABLE 2

COMPILATION OF PROPERTIES FOR 55 CLUSTERS

cluster	Z	V_{disp} (km s^{-1})	R_c^{opt} (Mpc)	R_{core}^{x-ray} (Mpc)	$N_{2.0}$	$N_{1.0}$	$N_{0.5}$	Center (x,y)	L_X (10^{43})	M_{gas} (10^{13})
(1)	(2)	(3)	(4)	(5)	(6)	(7)	(8)	(9)	(10)	(11)
A14	0.0640	—	0.57	—	93.0	37.0	18.7	146,96	—	—
A76	0.0416	—	0.23	0.409	58.6[a]	30.6	9.8	161,163	4.53	6.57
A119	0.0440	778	0.83	0.324	102.7[a]	46.1	22.4	168,170	22.8	14.0
A151	0.053	715	0.73	—	66.5	41.4	23.2	245,254	—	—
A154	0.0658	999	0.80	0.170	75.6	48.1	32.8	139,92	7.42	6.69
A168	0.0452	581	0.24	—	91.8[a]	42.6	10.9	114,181	6.62	6.50
A194	0.0178	440	0.38	0.195	43.0[a]	22.9	11.4	243,240	1.33	2.74
A376	0.0489	—	1.05	0.037	127.9[a]	66.5	34.3	139,100	11.2	8.50
A400	0.0232	610	0.43	0.160	53.3[a]	27.6	13.3	243,237	4.03	4.78
A496	0.0320	714	0.39	0.135	63.2[a]	34.9	13.7	171,170	31.9	11.5
A539	0.0205	701	0.56	0.135[b]	56.8[a]	31.3	18.9	234,237	5.17	4.30
A548	0.0410	872	0.69	0.185	94.2[a]	45.8	21.9	133,294	7.43	7.44
A592	0.0624	—	0.26	0.145	37.0	19.4	9.4	243,245	8.57	6.00
A754	0.0528	880	0.71	0.575[c]	68.1	37.6	18.8	210,233	68.7	21.5
A838	0.051	—	0.26	—	23.7	10.4	4.8	253,178	—	—
A957	0.0440	678	0.56	0.144	43.3	29.1	18.2	270,238	5.91	6.12
A978	0.053	—	0.17	—	39.6	14.7	6.6	249,239	—	—
A979	0.055	—	0.23	—	52.2	22.0	5.2	252,240	0.42	—
A993	0.053	—	0.29	—	35.4	20.1	7.0	245,272	—	—
A1069	0.063	—	0.28	—	24.0	16.1	7.1	163,156	—	—
A1139	0.038	—	0.16	—	40.2	17.4	6.3	307,263	—	—
A1142	0.0353	417	0.28	0.195	23.7[a]	12.6	6.0	249,238	1.76	2.99
A1185	0.0304	783	0.39	0.150[b]	32.2[a]	17.1	11.0	161,158	2.71	3.23
A1377	0.0514	488	0.42	0.288	44.5	29.8	14.1	134,143	4.70	5.73
A1631	0.0508	711	0.52	0.71[c]	86.4	44.8	16.8	243,257	5.22	8.18
A1644	0.0449	991	0.20	—	85.1	31.7	7.6	251,234	24.9	11.1
A1656	0.0232	880	1.24	0.430[b]	150.4[a]	79.5	40.4	254,233	68.0	21.6
A1736	0.0431	783	0.10	0.400[b]	96.8	37.0	11.9	237,237	13.9	8.87
A1913	0.0533	656	0.61	0.566	52.1	30.0	17.2	272,276	5.81	8.00
A1983	0.0441	504	0.60	0.081	72.7	34.0	19.6	233,246	3.52	3.22
A1991	0.0586	510	0.25	0.059	43.9	20.9	4.6	243,253	16.4	6.88
A2040	0.0456	—	0.48	0.139	54.4	31.0	15.2	244,250	3.44	3.84
A2063	0.0337	652	0.76	0.172	67.6	44.0	22.4	244,238	17.4	8.47
A2151	0.0371	786	0.29	—	83.7	31.5	11.4	297,237	8.76	4.45
A2256	0.0601	1270	1.05	0.444[b]	141.8[a]	65.8	32.8	89,50	79.0	22.0
A2589	0.042	500	0.72	—	75.5[a]	37.8	24.4	140,87	—	—
A2634	0.0312	976	0.98	0.420	129.8[a]	60.3	22.8	97,141	6.93	7.80
A2657	0.0414	667	0.73	0.139	75.5[a]	39.3	19.1	109,140	17.0	10.2
DC0003	0.035	433	0.25	—	33.7[a]	18.5	8.0	175,234	—	—
DC0107	0.0230	679	0.26	0.297	31.4[a]	19.1	8.6	175,192	3.81	5.17
DC0103	0.023	—	0.10	—	26.3[a]	14.0	7.9	255,249	—	—
DC0247	0.021	465	0.42	0.037	31.6[a]	16.8	11.6	253,248	1.46	1.63
DC0317	0.055	—	0.30	—	44.4	22.1	11.1	252,217	—	—
DC0326	0.0593	—	0.10	—	67.0	32.2	10.7	267,214	1.86	—
DC0329	0.0554	—	0.95	—	140.8	59.6	21.3	289,198	14.7	7.85
DC0410	0.017	—	0.21	—	26.9[a]	14.3	4.6	239,241	—	—
DC0428	0.041	616	0.76	—	81.3	46.7	22.8	248,214	—	—
DC0559	0.049	780	0.64	0.460[c]	54.7	35.0	17.2	166,276	17.2	12.5
DC0608	0.035	282	0.52	—	60.4	36.3	16.0	250,277	—	—
DC0622	0.0265	—	0.51	0.375[c]	56.3[a]	26.7	16.1	236,262	3.28	5.38
DC1842	0.0141	551	0.50	0.157	59.2[a]	31.5	15.7	169,172	0.98	2.22
DC2048	0.046	854	1.12	—	129.7	68.4	23.0	209,169	—	—
DC2103	0.052	—	0.20	—	63.6	25.1	11.1	249,255	1.22	—
DC2345	0.027	—	0.68	—	85.5[a]	39.7	21.1	175,174	—	—
DC2349	0.028	—	0.10	—	44.4[a]	23.6	5.2	168,163	0.13	—

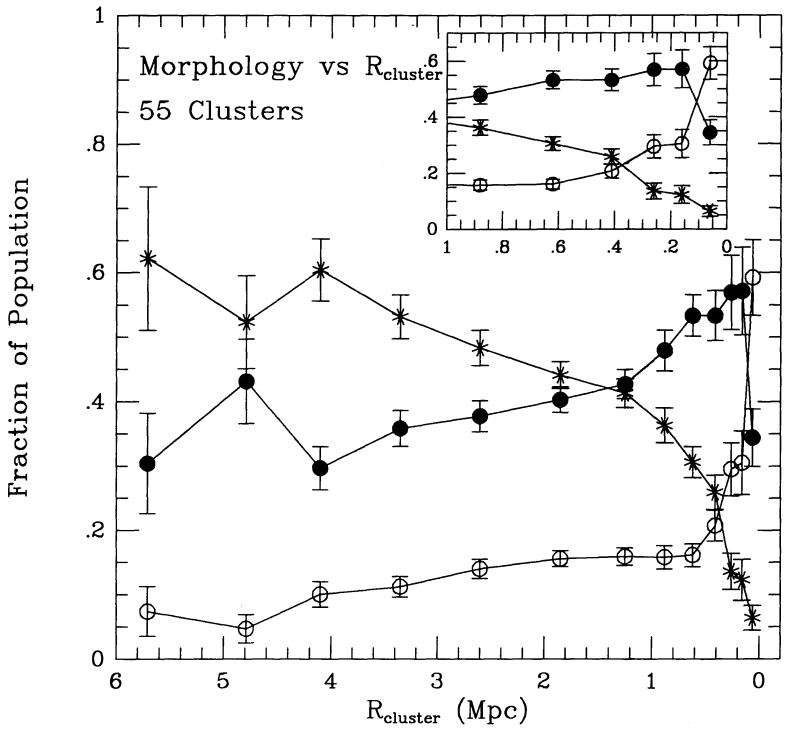

FIG. 4.—Morphology-clustercentric radius relation for all 55 clusters after corrections for the foreground/background contamination and magnitude cutoffs have been made.

pressure sweeping), it is possible that the same mechanism is affecting all three morphological types.

Figure 5 shows the same data but using the even-bins technique introduced in WG to allow direct comparisons between different correlations. This technique sorts the data by a given parameter and then divides the data into 20 even bins. The difference between the morphology-radius relation and the morphology-density relation is more apparent than in WG, with the elliptical fraction rising to a central value of 50% $\pm$ 4% as compared to 43% $\pm$ 4%. The drop in the S0 fraction near the center is only seen for the morphology-radius relation.

Figure 6*a* shows the morphology-radius relation normalized by R_c^{opt}. Figure 6*b* shows the relation normalized by $R_{core}^{X\text{-ray}}$, using only the 27 clusters where a one-component model provides a good fit (see Table 2). As expected, the normalization increases the elliptical fraction for the central bin, and makes the transition from the nearly flat outer gradient to the steep inner gradient even sharper, although both effects are very small. The primary usage of this normalization will be to provide a fair comparison between galaxies from different size clusters. The characteristic optical radius, R_c^{opt}, will be used throughout the rest of the paper, since we only have values of $R_{core}^{X\text{-ray}}$ for about half of the clusters.

Although tuning up the morphology-clustercentric radius relation shows that the correlations are better than with local density, the differences are still only at about the 2 σ level. In the following section we discuss a simple test which makes it more apparent that the morphology-clustercentric relation is the more fundamental correlation.

NOTES TO TABLE 2

Col. (2): Redshifts from Jones et al. 1993 when available, or Dressler 1980.

Col. (3): Cluster velocity dispersion from Struble & Rood 1991.

Col. (4): Characteristic cluster radius from the optical data, defined as the radius at which the cumulative number density falls below 20 galaxies Mpc^{-2}. Corrections for foreground/background contamination and the magnitude cutoff have been made. A minimum value of 0.10 Mpc was used for clusters that never reached a value of 20 galaxies Mpc^{-2}.

Col. (5): Core radius from the X-ray data (Jones et al. 1993).

Col. (6): The number of galaxies within 2.0 Mpc (H_0 = 50 km s^{-1} Mpc^{-1}) of the cluster center. Corrections for superposed galaxies and the magnitude cutoff have been made.

Col. (7): Same as col. (6) for 1.0 Mpc.

Col. (8): Same as col. (7) for 0.5 Mpc.

Col. (9): Position of cluster center in (X, Y) coordinate system of Dressler (1980). See text for more details.

Col. (10): X-ray luminosity within 1 Mpc of a center defined to obtain the maximum flux, in the range from 0.5 to 4.5 keV (Jones et al. 1993). Units are 10^{43} ergs cm^{-2} s^{-1}.

Col. (11): Mass of the X-ray gas within 2 Mpc of the center. Units are 10^{13} $M_\odot$.

[a] From an extrapolation based on clusters with similar number densities at smaller radii.

[b] A two-component model provides a slightly better fit; so this core radius, which is based on a one-component model, is probably slightly too high.

[c] A two-component model provides a much better fit; so this core radius, which is based on a one-component model, is too large.

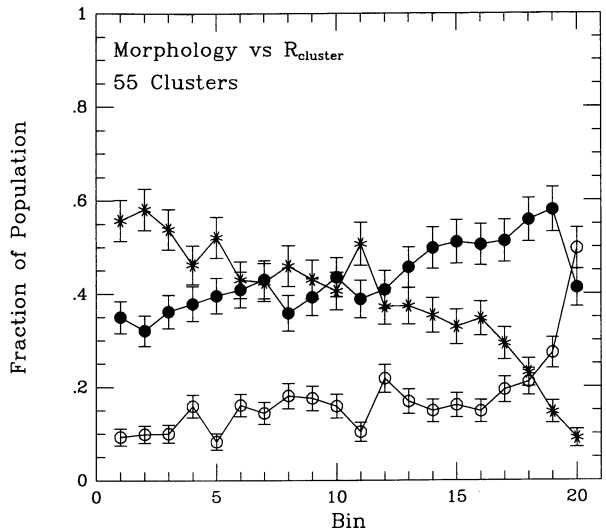

FIG. 5a

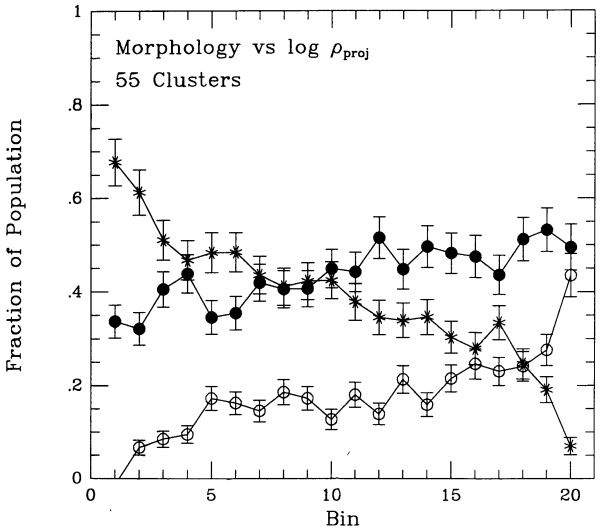

FIG. 5b

FIG. 5.—Morphology-clustercentric radius relation (*a*) and morphology-local density relation (*b*) for all 55 clusters. The even-bins technique is used. This provides a method of making a direct comparison between the two relations. We find that the morphology-radius relation results in stronger correlations, especially for the inner bin.

3.1. *Which is the Fundamental Parameter: Clustercentric Radius or Local Density?*

The projected local galaxy density correlates fairly well with the projected clustercentric position for most clusters. This makes it difficult to determine which of these is the more fundamental parameter. However, Figure 4 from WG shows that there is a large amount of scatter in the correlation. This provides some hope of decoupling the two dependencies. We have performed two tests designed to determine which is the more fundamental parameter.

3.1.1. *Same Local Density—Different Clustercentric Position*

In the first test we isolate regions with the same local density, but different clustercentric positions (i.e., the outermost region with a given local density and the innermost region with the same local density). If the morphology-density relation is the more fundamental correlation, these regions should have the same morphological fractions. The results were first reported in Whitmore (1991). We find that the elliptical fraction *rises* by about 15% for the inner regions, consistent with the morphology-radius relation.

A very interesting sidelight of this test was the discovery that very close pairs have a higher elliptical fraction than would be predicted by their position in the cluster. For example, for pairs with projected separations of less than 0.05 Mpc the elliptical fraction is 35%, even though the pairs are in the outer regions where the elliptical fraction is generally about 15%. Very close groupings with more galaxies (i.e., triplets, quartets,

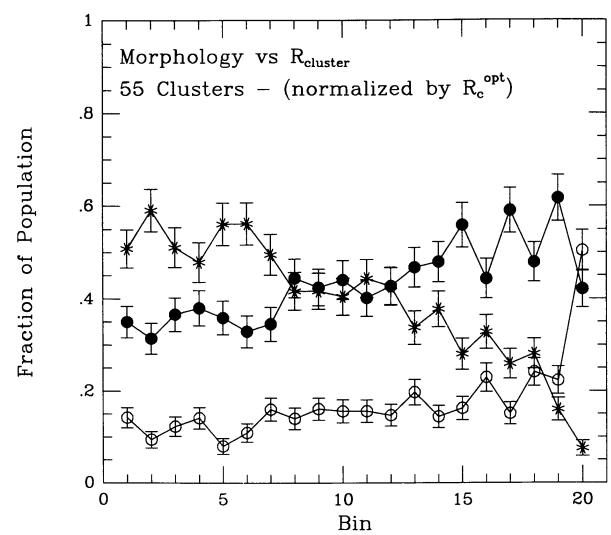

FIG. 6a

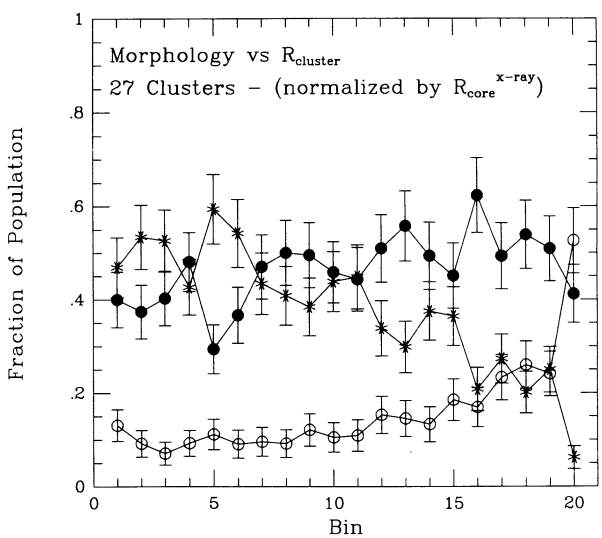

FIG. 6b

FIG. 6.—Normalized morphology-clustercentric radius relation for all 55 clusters. The clustercentric radius has been normalized (*a*) by a characteristic cluster radius, R_c^{opt}, where R_c^{opt} is the radius at which the cumulative projected density of galaxies drops below 20 galaxies Mpc^{-2}, and (*b*) by a core radius determined from the X-ray data, $R_{core}^{X\text{-}ray}$ (Jones et al. 1993).

etc.) show a similar, but much smaller, enhancement. J. Charlton (1992, private communication) also finds the enhancement in elliptical fraction for close pairs in the dense regions of the CFA redshift survey (i.e., primarily the Virgo cluster), but not in the isolated field. While the total CFA sample has an elliptical fraction of 7% ± 1.5%, the pairs with separations of less than 0.075 Mpc, and 400 km s^{-1}, have an elliptical fraction of 19% ± 5%.

While the enhancement in the elliptical fraction for close pairs and triplets may suggest the existence of a morphology–very local density relation, albeit only when very local density is defined by the nearest one or two galaxies, it represents only a minor modification of the overall elliptical fractions in clusters, since the number of galaxies in close pairs is relatively small. The procedure described above tends to highlight this difference, but only 7% of the galaxies which are more than 0.5 Mpc from the cluster centers are within 0.05 Mpc of another galaxy. If these galaxies are removed from the sample, the elliptical fraction only falls about 1% in this region (i.e., from 16% to 15%). The enhancement in the elliptical fraction for pairs is explored in more detail in Charlton, Whitmore, & Gilmore (1992). For the purposes of the present paper this effect will not be considered further. The main result of this first test, in terms of the topic of the current paper, is that the morphology-radius relation appears to be the more fundamental relation.

3.1.2. *Same Clustercentric Position—Different Local Density*

For this test we consider only the innermost galaxies (i.e., with $R/R_c^{opt} < 0.25$). Figure 7 shows the normal morphology-density relation for this subsample of 253 galaxies. The solid lines show the predictions for the morphology-density relation, while the dashed lines show the predictions for the morphology-radius relation. The data clearly favor the morphology-radius relation. Only for the lowest density point is there a slight hint that the elliptical fraction may be dropping, probably because of the inclusion of a few clusters which are actually the outskirts of another cluster (see § 2.5).

Figure 7 provides dramatic proof that clustercentric position is the fundamental parameter and suggests that the success of the morphology-density relation results from the generally good correlation between local density and clustercentric position. In the following sections we will examine whether the normalized radius, R/R_c^{opt}, is the only parameter which is involved, or whether the morphological fractions also depend on central number density, velocity dispersion, or X-ray flux.

3.2. *Correlations with $N_{0.5}$*

In this section we test whether the morphology-clustercentric radius relation depends on the central number densities by breaking the sample into four subsamples according to the number of galaxies within 0.5 Mpc of the cluster center, $N_{0.5}$.

Figure 8 shows the result using the even-bins technique. We find a clear separation in the morphology-radius relations, with the low-density clusters showing a smaller elliptical enhancement near the center. While this is the relevant figure when determining the overall enhancement in the *number* of ellipticals, it does not prove that the elliptical enhancement is not present at the very center of low $N_{0.5}$ clusters, since the inner bin covers a much wider range in radius for the low $N_{0.5}$ clusters (0–0.47 Mpc) than for the high $N_{0.5}$ clusters (0–0.30 Mpc). In addition, the low $N_{0.5}$ clusters have much smaller values of R_c^{opt} than the high $N_{0.5}$ clusters, so the 0.47 Mpc figure represents the outer regions of these clusters. These two effects make the comparison between the subsamples invalid.

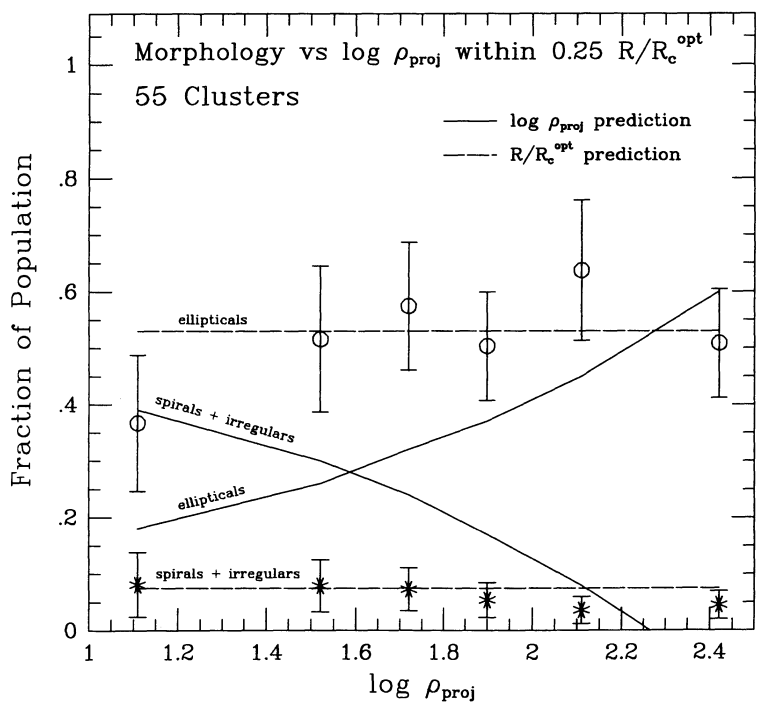

FIG. 7.—Morphology-density relation for the galaxies within $0.25R/R_c^{opt}$ of the cluster centers. Solid lines are the predictions for the morphology-density relation; dashed lines are the predictions for the morphology-radius relation. Only the ellipticals and the spiral + irregular galaxies are shown for clarity. The data clearly favor the morphology-radius relation.

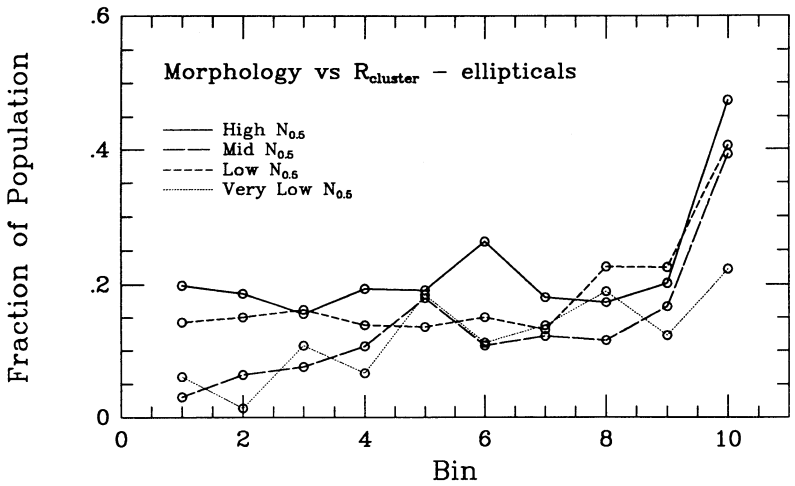

FIG. 8*a*

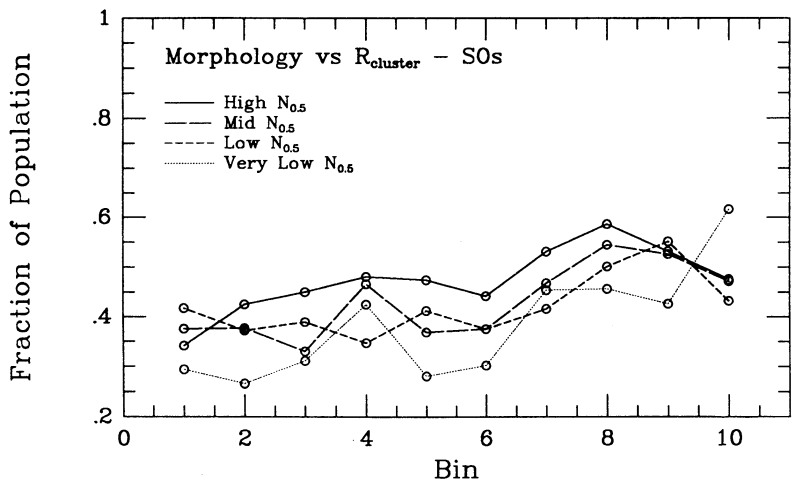

FIG. 8*b*

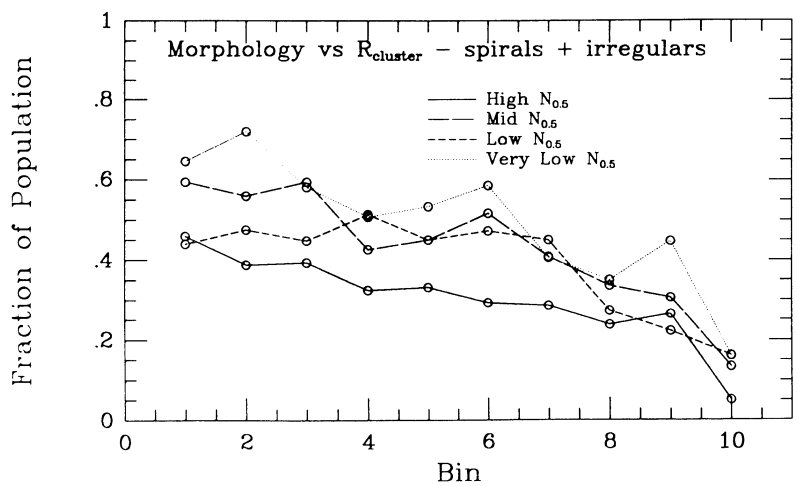

FIG. 8*c*

FIG. 8.—Morphology-clustercentric radius relation for subsamples with different values of the central number density, $N_{0.5}$. The even-bins technique is used. Note how the clusters with large central number densities have a much larger enhancement of elliptical galaxies than the clusters with low central number densities.

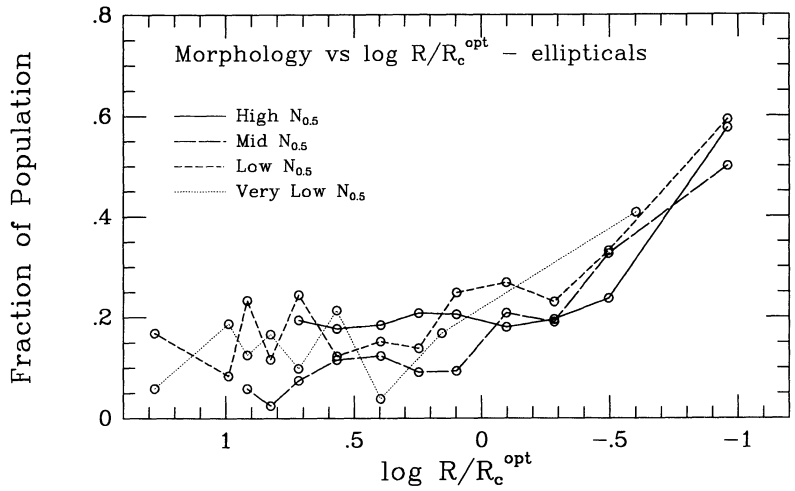

FIG. 9*a*

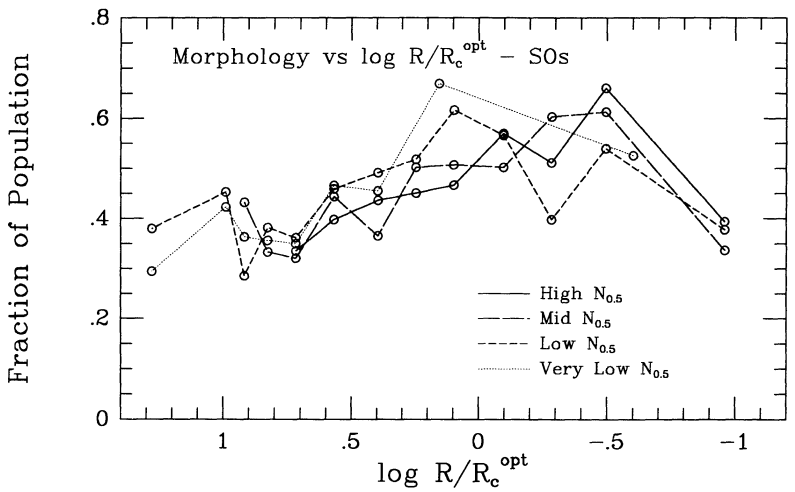

FIG. 9*b*

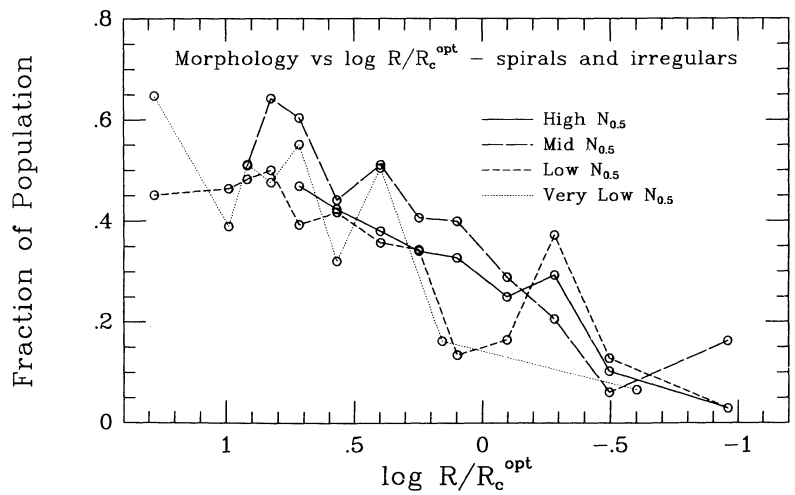

FIG. 9*c*

FIG. 9.—Normalized morphology-clustercentric radius relation for subsamples with different values of the central number density, $N_{0.5}$. The mean values for the four bins were 6.9, 12.4, 18.4, and 26.9 galaxies. We find the same relation for all clusters (i.e., even the low $N_{0.5}$ clusters have a high elliptical fraction near the very center of the cluster, although the number of galaxies in this normalized region is much smaller than for a cluster with a large value of $N_{0.5}$).

Figure 9 shows the same data but with the radius normalized by R_c^{opt}. A log radius scale is used in the figure to help show the behavior in the inner regions, but we should keep in mind that the gradients actually change very rapidly near the center. All four subsamples now follow the same curves! The observed scatter is almost exactly what would be expected based on the number of galaxies in each bin. Even for very sparse clusters, at the very center the elliptical fraction is quite high. Similarly, the elliptical fraction in the outer regions of clusters is always low, even in what are generally considered to be "elliptical-rich" clusters. It appears that it is only necessary to know a single parameter, R/R_c^{opt}, in order to predict the morphological fractions in clusters.

Another interesting result is that the spiral fraction is falling for all four subsamples and is nearly zero at the cluster center. Spirals have a difficult time living in the central regions of all clusters, even very sparse clusters.

We also broke the sample into four subsamples based on the ratio $N_{0.5}/N_{1.0}$. This provides a crude concentration estimate for the clusters. The result was virtually indistinguishable from Figure 9 (i.e., all four subsamples show the same normalized morphology-radius relation).

3.3. *Correlations with Velocity Dispersion*

Velocity dispersions are available for 35 of the clusters, and are listed in Table 2. Figure 10 shows the data for three subsamples based on velocity dispersion, V_{disp}. We again find essentially no separation in the normalized morphology-radius relation, supporting our earlier conclusion that only one parameter, R/R_c^{opt}, is needed to predict the morphological fractions.

3.4. *Correlations with X-Ray Flux*

X-ray luminosities (L_X; luminosity within the 0.5–4.5 keV range) are available for 39 of the clusters (Jones et al. 1993). Figure 11 shows the normalized morphology-radius relation for three subsamples ranked in order of L_X. Once again we find essentially no separation in the morphological gradients.

Although computing the morphological fractions at each radius is useful for determining the relative morphological mix, it obscures what is actually happening to the density profile in the cluster for each morphological type. Figure 12 shows the density profiles for each of the L_X subsamples. The radii have been normalized by R_c^{opt}. We find that as we approach the cluster center the density profile for the spirals is much flatter than the profile for the S0 or elliptical galaxies. In fact, the gradient is actually falling for the high L_X clusters. Once again it appears that spiral galaxies have a difficult time existing near the centers of clusters.

4. A SIMPLE MODEL FOR THE ORIGIN OF MORPHOLOGICAL FRACTIONS IN CLUSTERS OF GALAXIES

4.1. *Motivation*

Current models which attempt to explain the morphological mix via biasing in cold dark matter simulations fail to predict the nearly flat outer gradient in the elliptical fraction, and the rapid increase inside 0.5 Mpc. These models have the added problem of explaining why the gradients in the elliptical fraction are so different from the gradients in the spiral and S0 fractions. For example, while Evrard, Silk, & Szalay (1990) find that they can produce a reasonable fit to the morphology-density relation for ellipticals (it is unclear whether they will be able to produce the sharp rise in the morphology-radius relation), their fits to the spiral and S0 gradients are very poor. While the observed S0 fraction increases in a nearly linear fashion from 28% in the lowest density regions to 47% in the highest density regions (Dressler 1980), the prediction from the Evrard et al. model is for a nearly constant fraction at about 33% for this range. The poor agreement of their model with the S0 and spiral fractions is partially obscured by the combination of S0 and elliptical galaxies in their model (e.g., see their Fig. 6).

Several of the correlations discussed in § 3 point an accusatory finger toward the cluster centers as the primary cause of morphological segregation in clusters. These include (1) the sharp rise in the elliptical fraction at about 0.5 Mpc, (2) the sharp decline in the S0 and spiral fractions within 0.2 Mpc of the center, and (3) the fact that the cluster density profile for spirals is actually falling in the centers of most clusters. *This information provides clear evidence that some mechanism which is unique to the center of the cluster favors the existence of ellipticals rather than disk galaxies.* This argues for a hybrid model, where initial conditions are responsible for the morphological mix in the outer regions of the cluster, and in the field, but some evolutionary effect modifies these fractions near the centers of clusters.

There are two ways to increase the fraction of elliptical galaxies in the centers of clusters. We can either make more elliptical galaxies or we can make fewer spiral and S0 galaxies. *The fact that spiral galaxies predominate in most regions of the universe, but are essentially absent at the very centers of rich clusters, suggests the latter possibility is the correct choice. The centers of clusters represent a very hostile environment for the slow formation of a disk (i.e., strong tidal shear from the mean field of the cluster, high density of rapidly moving galaxies, presence of X-ray gas, cannibalism by the D galaxy). This leads us to conclude that destructive processes are responsible for controlling the morphological fractions in cluster centers rather than formation processes.*

If the destruction of spiral and S0 galaxies is required to increase the elliptical fraction near the center, the obvious question is where does the material from the failed galaxies end up. The lack of a bright intracluster medium in visible light requires most of the material to still be in a gaseous state when the galaxies were destroyed (i.e., most galaxies were still protogalactic gas clouds). A reasonable assumption would therefore be that the material ends up forming the hot intracluster medium. In this case we might expect the enhancement of elliptical galaxies to correlate with the X-ray properties of the clusters.

When combined with the assumption that the intrinsic fraction of elliptical galaxies is about 10%, and the assumption that ellipticals formed very early and therefore survived the cluster collapse, this simple model leads to a large number of testable predictions, as we shall see in the following sections. While the exact physical mechanism need not be specified for the model, tidal disruption by the mean field of the cluster is an attractive option since tidal forces vary as R^{-3}. Since the mass of the cluster increases roughly as R, the tidal shear would decrease as R^{-2}, possibly explaining the sharpness of the rise in the elliptical fraction. This possibility is examined in more detail in § 4.4.

Our scenario has aspects suggested by several other studies. For example, Eggen, Lynden-Bell, & Sandage (1962), Gott & Thuan (1976), and Gunn (1982) have argued that spheroidal

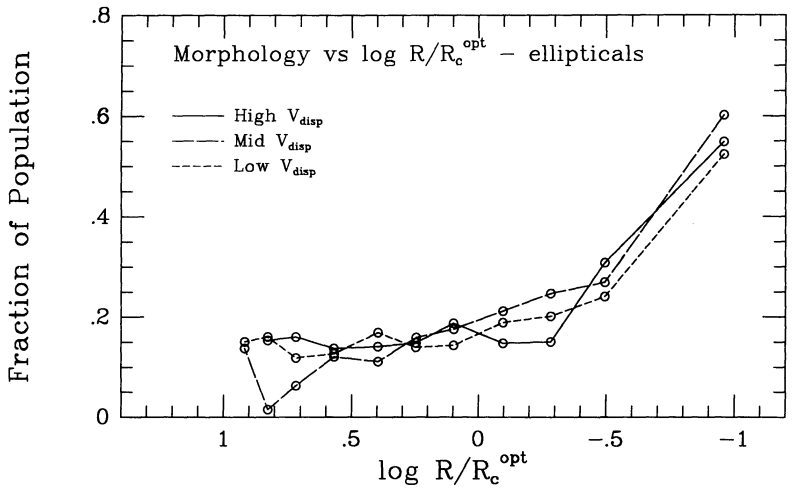

FIG. 10*a*

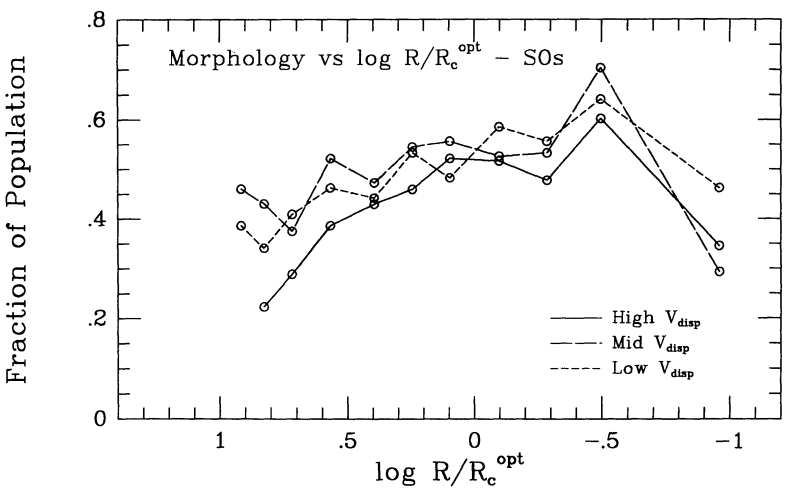

FIG. 10*b*

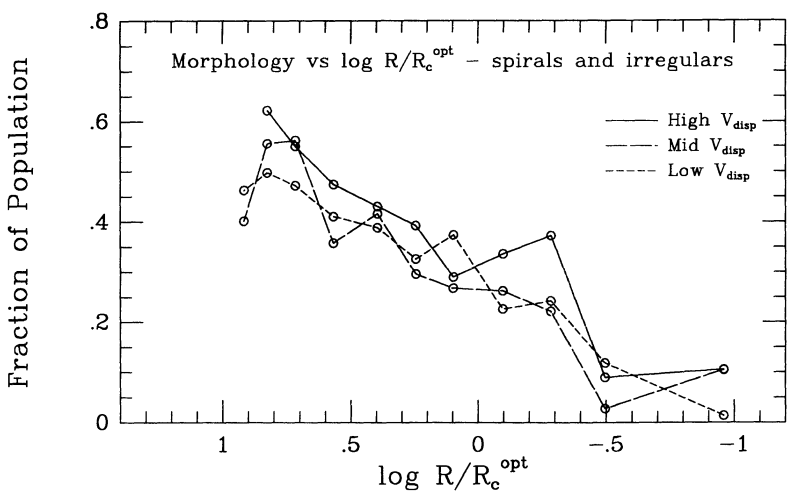

FIG. 10*c*

FIG. 10.—Normalized morphology-clustercentric radius relation for subsamples with different values of the cluster velocity dispersion, V_{disp}. The mean values for the three bins were 504, 720, and 945 km s^{-1}.

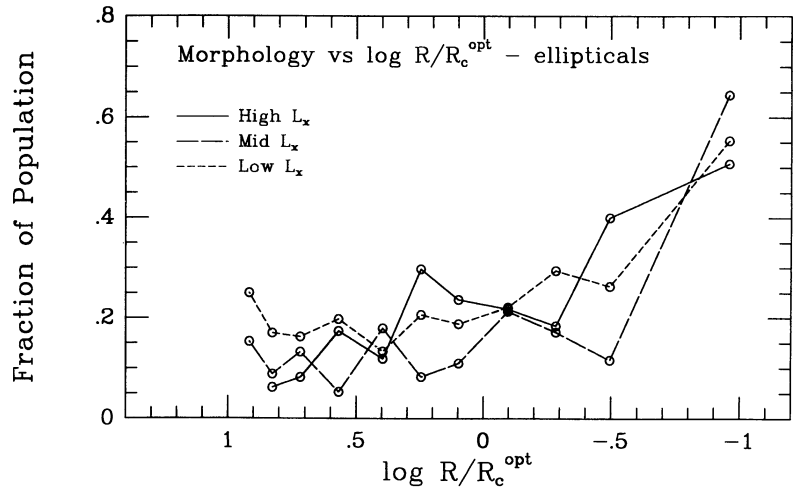

FIG. 11*a*

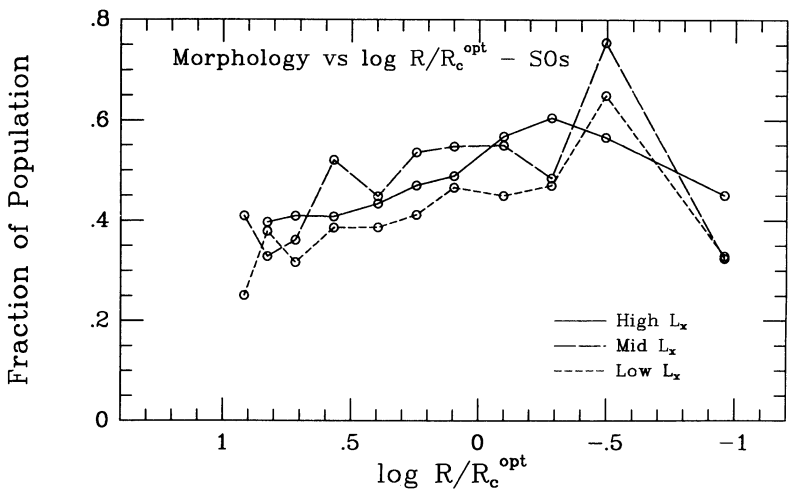

FIG. 11*b*

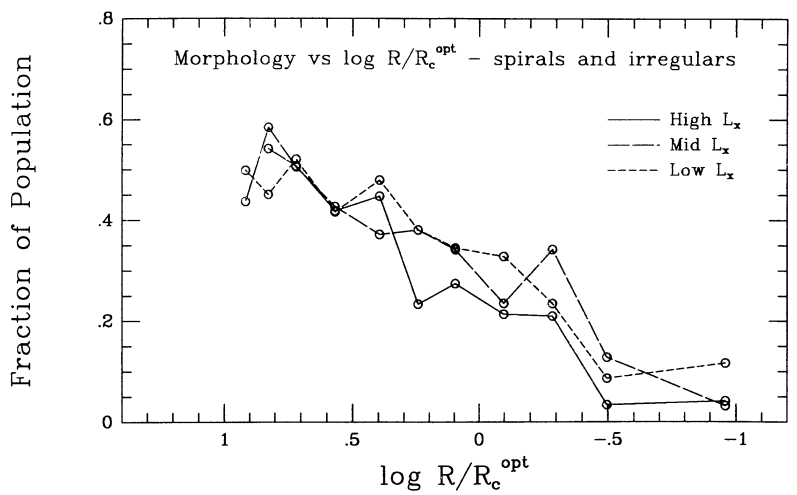

FIG. 11*c*

FIG. 11.—Normalized morphology-clustercentric radius relation for subsamples with different values of the X-ray luminosity, L_X. The mean values for the three bins were 2.3, 7.5, and 34.4 ergs cm^{-2} s^{-1}.

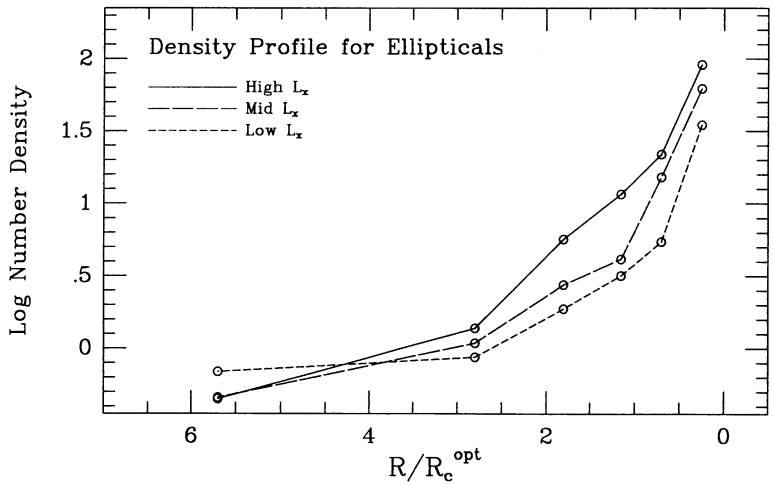

FIG. 12*a*

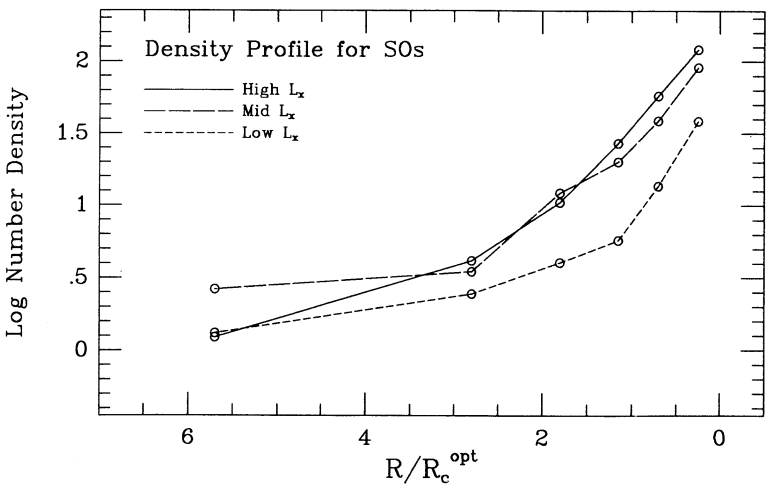

FIG. 12*b*

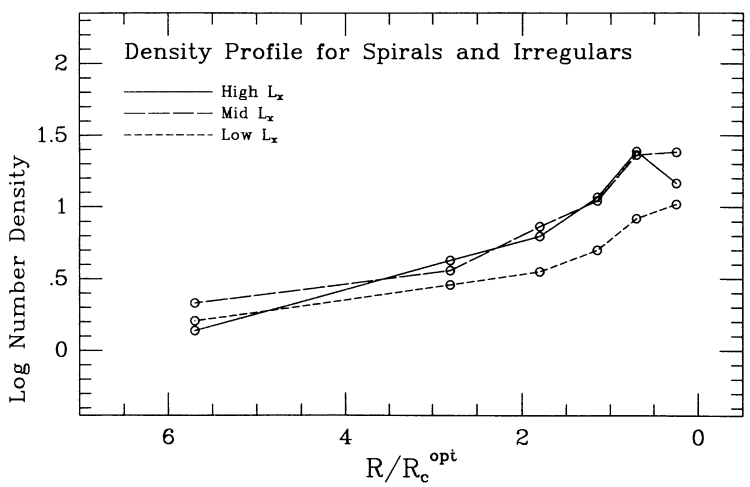

FIG. 12*c*

FIG. 12.—Number density profile for the system (*a*) ellipticals, (*b*) S0's, and (*c*) spiral and irregular galaxies as a function of the L_X subsamples. Note how much flatter the profile is for the spiral and irregular galaxies. The profile is actually falling near the center of the high L_X clusters.

components should form first, with the infall of the disk occurring on a longer time scale. Larson, Tinsley, & Caldwell (1980), Gunn (1982), Meisels & Ostriker (1984), and Postman & Geller (1984) have all suggested that truncated star formation by the removal of a gaseous halo in cluster environments could modify the evolution of disk galaxies. Tully & Shaya (1984) and Shaya & Tully (1984) have developed a model where the tidal field of the Local Supercluster determines the morphology of the galaxies. Binney (1980) argued that the intracluster medium was formed by protodisk material which was disturbed by the overall collapse of the cluster. What is new in our treatment is the comparison with the morphology-clustercentric radius relation and the direct tie-in with the X-ray properties of the cluster.

4.2. *A Description of the Model*

The model is defined by the following three basic assumptions:

1. *The intrinsic morphological mix is* $E/(S0 + S + I) = 10\%/90\%$. These are roughly the fractions found in the outer parts of clusters (§§ 2 and 3) as well as in loose groups and in the field (Postman & Geller 1984; Rood & Williams 1989). These fractions are appropriate for a magnitude cutoff of -20.4 in V.

2. *The relative order of formation is elliptical galaxies first, cluster collapse next, S0 galaxies next, and spiral and irregular galaxies last.*

(a) *Most elliptical galaxies form first.* The near constancy in the colors of most ellipticals (Bower, Lucey, & Ellis 1991), as well as their spectral makeup (Wyse 1985), provides evidence that most ellipticals formed at a very early epoch. Larson (1990) estimates that the bulk of star formation in luminous spheroids was at around $z = 5$ or earlier. The basic picture suggested by several studies (e.g., Gott & Thuan 1976) is that the largest density enhancements collapse first and form elliptical galaxies. In our model, these galaxies are treated as hard "nuggets" that the subsequent cluster collapse cannot destroy.

(b) *The cores of most clusters collapsed next.* The era of cluster collapse is quite extended and is still occurring in the outer regions of most clusters. Maoz (1990) estimates that the Coma cluster collapsed at $z = 2.4$–8.5. The smaller values are for $\Omega = 1$. Collapse times for clusters with velocities dispersions more typical of our sample would be in the range $z = 1.6$–5.7.

(c) *S0 galaxies formed next.* S0 galaxies formed from smaller density enhancements than elliptical galaxies, hence, they take longer to collapse. The bulge forms first, in a manner quite similar to the formation of ellipticals, with the gas remaining in the outer protogalactic halo slowly settling into a disk. S0s have bulge magnitudes that are intermediate between ellipticals and spirals since they formed from intermediate density enhancements.

(d) *Spiral and irregular galaxies formed last.* Spiral and irregular galaxies formed from still weaker density enhancements, with the Sa galaxies forming first from slightly larger density enhancements and the Sc and Irregular galaxies forming last. Larson (1990) estimates that our disk formed at $z = 1$–1.5.

3. *During the collapse of the cluster core, any remaining protogalactic clouds are destroyed.* Only galaxies that have collapsed and formed stars survive the cluster collapse. The material from the failed galaxies produces the intracluster medium in the cluster and is observed as the X-ray halo.

Several modifications to this very simple model can be envisioned. For example, we have assumed that all of the gas in the intracluster medium was originally destined to become spiral and S0 galaxies, although it is probably more reasonable to assume that some fraction of the gas was actually left over from galaxy formation. Our approach will be to see how well the simple model works, and if necessary, use the discrepancies to provide guidance on what types of modifications are required.

4.3. *A Qualitative Explanation for Various Observations*

The model was originally developed to provide a framework for understanding the morphology-clustercentric radius relation (Fig. 4). In this section we discuss how the model can also provide a qualitative explanation for various other observations. In the following section we will make quantitative estimates, where possible.

1. The gas-to-stars ratio is larger in rich clusters than in poor clusters (David et al. 1990; Arnaud et al. 1992).

In any biasing picture, regions with higher mass density should form more stars and galaxies. The gas-to-stars ratio should therefore be smaller in rich clusters. David et al. (1990) and Arnaud et al. (1992) find that the reverse is true; the richest clusters have the highest fraction of their mass in the form of gas. This seems to indicate that galaxy formation is less effective in rich clusters. However, from our viewpoint we would say that destruction mechanisms have been *more* effective in rich clusters, a natural consequence of the model.

Ginga observations by Hatsukade (1989) and David, Forman, & Jones (1991) show a change in the iron abundance in the intracluster medium of rich clusters. Arnaud et al. (1992) also report that the iron mass in the intracluster medium decreases with cluster richness, as would be expected if a larger fraction of the protogalaxies, with their unprocessed gas, were destroyed in rich clusters. In this picture, most of the iron enriched material comes from the ellipticals and S0s that formed earliest, while the destroyed protogalaxies act to dilute the intergalactic medium.

2. The density of spiral galaxies is relatively constant near the centers of clusters. For high-L_X clusters, the density of spirals is actually falling (Fig. 12).

Figure 12 shows that the density profile for the system of spiral galaxies is nearly flat for most clusters, unlike the density profile for the system of S0s or ellipticals which are rapidly increasing. For high L_X clusters the density profile is actually falling near the center! This provides strong evidence that spirals are not able to form near the centers of high L_X clusters, as assumed in the model.

Bingelli, Tammann, & Sandage (1987, Fig. 16) find a similar flattening for the density profile of spiral and irregular galaxies in the Virgo cluster. The density profile would have actually declined in the inner regions if M87 had been used as the cluster center. Bingelli et al. also find a hole in the distribution of Im galaxies near the center of the Virgo cluster.

3. The gradients for Sa galaxies are flat while the gradients for Sc galaxies are falling (Fig. 13).

In our model, the larger the spheroidal component (i.e., the bulge for spiral and S0 galaxies), the earlier the galaxy formed.

The earlier the galaxy formed, the better chance it has to withstand the cluster collapse. We would therefore expect Sa galaxies to have relatively flat gradients in the outer regions, similar to S0 galaxies, while Sc galaxies should have strong negative gradients. Figure 13 shows that this is the case.

We also find that all three types of spirals are missing at the centers of the clusters, where the tidal shear is the strongest. The "strength" of the sharp decline near the center is correlated with the time sequence of formation, as expected (i.e., S0 galaxies have the smallest decline, followed by Sa, Sb, and Sc galaxies).

4. S0 galaxies have larger bulges than spiral galaxies (Dressler 1980).

Dressler has raised this as an objection to the idea that ram-pressure sweeping has converted spirals into S0 galaxies. In our model the larger bulges result from our assumption that S0 galaxies formed earlier than spirals due to the higher density enhancement, and hence larger bulge component. The earlier a galaxy forms, the faster it uses its gas and becomes an S0. We therefore expect galaxies with the largest bulges to have the least current star formation, as observed.

5. The elliptical fraction in compact groups is only slightly higher than in the neighborhoods around the groups (Rood & Williams 1989; Sulentic 1987).

Compact groups of galaxies have space densities which are as high or higher than even the densest regions of clusters, so we might expect the compact groups to consist of essentially all elliptical galaxies, based on the morphology-density relation. This is not the case, however (see Mamon 1986, Fig. 2, and Hickson, Kindl, & Huchra 1988).

Our model would predict a low elliptical fraction since the galaxies did not go through a large cluster collapse early in their evolution. A collapse of the compact group with fewer galaxies involved would have less effect on the spiral and S0 populations since they have already formed.

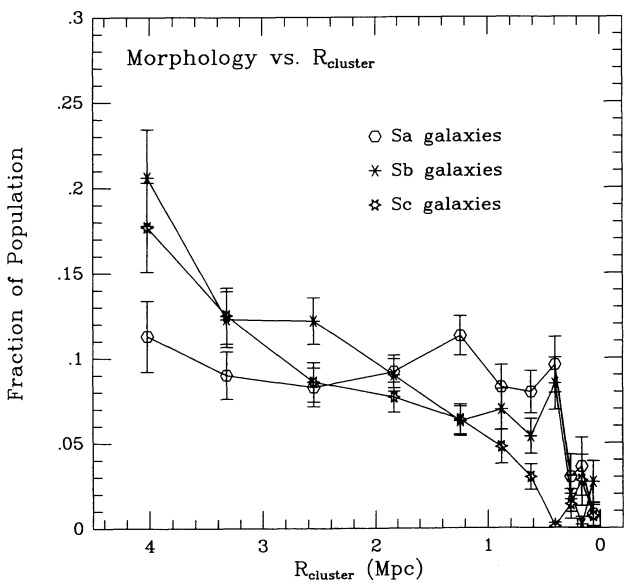

FIG. 13.—Morphology-clustercentric radius relation for Sa, Sb, and Sc galaxies. A few Sd galaxies are also included with the Sc galaxies. Note the similarity between the gradient for Sa and S0 galaxies, and the steep slope of the Sc galaxies. The region of exclusion near the center of the cluster is much larger for the Sc galaxies than for the Sa galaxies.

6. The morphology-density relation is very weak, or nonexistent, in compact groups, loose groups, and in the field (Whitmore 1992).

In a recent review, Whitmore (1992) examines the evidence for a morphology-density relation in various environments. Hickson et al. (1988) find a very weak relation for compact groups, in contrast to the correlation between morphology and group velocity dispersion which is quite strong. This again argues that a deep potential well, hence large velocity dispersion, is needed to increase the elliptical fraction.

For loose groups, the Postman & Geller (1984) results were compromised by the inclusion of cluster galaxies in the sample (i.e., the densest "groups" tend to be galaxies from the centers of clusters such as Virgo and Coma). Plotting the morphology-density relation for the Geller-Huchra (1983) groups shows no correlation, similar to the results of Maia & Da Costa (1990) for loose groups selected from the Southern Sky Redshift Survey.

In the field, Huchra et al. (1990) find that outside the core of the Coma cluster, the distribution of early- and late-type galaxies is essentially the same in the CfA redshift sample. This is confirmed by Babul & Postman (1990) who find that the angular correlation function for early- and late-type galaxies is the same once the Coma cluster is removed. It appears that the only location where the morphological fractions are strongly modified is near the centers of clusters.

7. Galaxies within about 1 Mpc of the cluster center have falling rotation curves (Whitmore, Forbes, & Rubin 1988).

Some spirals that were formed in the inner regions before cluster collapse may be able to survive, but will probably lose their outer material due to the tidal shear. Similarly, a spiral that is falling into the cluster center for the first time may lose its outer material due to the present conditions in the cluster center. This may result in falling rotation curves, as found by Whitmore et al. (1988) for spirals within 1 Mpc of the cluster centers.

More recent studies by Distefano et al. (1990) and Amram et al. (1992) have only partially supported this finding, with much shallower correlations between the outer gradient of the rotation curves and the radius from the cluster center. This may simply be due to the fact that their samples have relatively more galaxies at large values of the clustercentric radius, R, and fewer galaxies within 1.0 Mpc of the cluster centers. Whitmore et al. fit a simple straight line to the data in their sample, all but one of which were within 3 Mpc of the cluster center. Taken at face value, this would imply very rapidly rising rotation curves at large values of R. However, a more reasonable interpretation is that there is only a correlation between the outer gradient of the rotation curve and R within about 1.0 Mpc of the center, beyond which the value of the outer gradient is constant, with the same value as seen in field galaxies (i.e., about 10%). Since most of the galaxies in the Amran et al. sample are beyond 1 Mpc (0.66 Mpc in their diagram since they use a Hubble constant of 75 km s^{-1} Mpc^{-1}), only a weak correlation would be expected, and is actually observed at about the 3 σ level.

8. Sa galaxies in clusters tend to be H I–deficient, rather than Sc galaxies (Dressler 1986).

In the model, protogalactic clouds that would eventually form Sc galaxies are destroyed, at least for the clouds that participate in the collapse of the cluster core. We therefore expect most current Sc galaxies to be from regions that did not

participate in this cluster collapse (i.e., reside in the outer regions or are falling in for the first time). Few of these will have ever been near the cluster center and hence few of them will have suffered ram-pressure sweeping. On the other hand, some Sa galaxies which formed earlier may have survived the cluster collapse. They may therefore be in orbits which take them near the cluster center and through the X-ray gas relatively often. These are the galaxies that we expect to be H I–deficient. Dressler (1986) also finds that the system of H I–deficient galaxies have lower velocity dispersions than the H I–rich galaxies. This again suggests that the H I–rich galaxies did not participate in the cluster collapse and have orbits that tend to keep them out of the cluster center.

4.4. *A Quantitative Comparison with the Observations*

It is possible to make quantitative checks on some aspects of the model. Other aspects will require more detailed simulations before a comparison can be made.

4.4.1. *The Mass of the X-Ray Gas*

The most basic prediction of the model is that the amount of X-ray gas in a cluster should match the amount of mass produced by "failed" spiral and S0 galaxies, as determined from the enhancement in the elliptical fraction near the centers of clusters. This is a very straightforward calculation with essentially no unknown parameters. We will adopt a value of 10% for the intrinsic value of the elliptical fraction, as justified in § 4.2. The number of failed spiral and S0 galaxies is determined by multiplying the elliptical enhancement above this 10% out to a radius of 2.0 Mpc by the number of galaxies within this radius. For example, in Figure 8 the average elliptical fraction within 2 Mpc of the cluster center is 23.59% for the high $N_{0.5}$ sample. The average number of galaxies within 2 Mpc of the center is $N_{2.0} = 106.4$ for these clusters. The number of failed spiral and S0 galaxies required to lower the elliptical fraction of 10% would therefore be $(23.59 - 10.0)/10.0 \times 106.4 = 144.6$ galaxies. A value of $6 \times 10^{10}\ L_\odot$ will be used as the luminosity of a typical galaxy, as determined from the observed luminosity function for clusters within $z = 0.035$. A correction term of 1.54 is used to extrapolate to galaxies dimmer than the cutoff magnitude of -20.4, based on the cumulative luminosity functions shown in Figure 2, plus the luminosity function for Virgo at dimmer magnitudes (Bingelli et al. 1987). The use of a Schechter (1976) luminosity function with $M_V^* = -21.7$, and $\alpha = -1.25$ gives essentially the same value. The missing luminosity is converted to mass by assuming a value of $M/L = 6$. This is an average value for S0 through Sc galaxies (Faber & Gallagher 1979). The final calculation for the high $N_{0.5}$ subsample would therefore be $144.6 \times 1.54 \times 6 \times 10^{10} \times \upsilon = 8.02 \times 10^{13}\ M_\odot$ for the mass of the X-ray gas. The calculations for the other subsamples are included in Table 3.

Figure 14 shows the prediction for $M_{\text{X-ray gas}}$ based on the elliptical enhancement for the $N_{0.5}$, V_{disp}, and L_X subsamples. The observed mass of the X-ray gas within 2.0 Mpc of the cluster center is shown as the solid line (Jones et al. 1993). We find that our predictions are only slightly lower than the observed values of $M_{\text{X-ray gas}}$, and even the slope of the correlation is roughly correct. The dotted line shows what our predictions would be if a value of 5% had been used for the intrinsic elliptical fraction.

Taken at face value, the fact that the predicted values are slightly lower than the observed value might lead us to conclude that the intrinsic elliptical fraction was about 7.5%. However, it is just as likely that the simplistic nature of the model is responsible for the gap. For example, we have assumed that all the material in the intracluster medium is produced by failed spiral and S0 galaxies. It is quite likely that

TABLE 3

ESTIMATE OF $M_{\text{X-ray gas}}$ FROM THE ELLIPTICAL ENHANCEMENT

Subsample (1)	N[a] (2)	$E\%_{2.0}$[b] (3)	Δ[c] (4)	$N_{2.0}$[d] (5)	Constant[e] ($M_\odot$) (6)	$M_{\text{X-ray gas}}$[f] ($M_\odot$) (7)
Large $N_{0.5}$	13	23.59%	1.359	106.4	5.54×10^{11}	8.02×10^{13}
Medium $N_{0.5}$	13	16.61	0.661	66.1	5.54×10^{11}	2.42×10^{13}
Low $N_{0.5}$	14	20.46	1.046	58.0	5.54×10^{11}	3.36×10^{13}
Very low $N_{0.5}$	15	16.03	0.603	39.3	5.54×10^{11}	1.31×10^{13}
Large V_{disp}	9	20.28	1.028	106.5	5.54×10^{11}	6.07×10^{13}
Medium V_{disp}	12	19.12	0.912	63.5	5.54×10^{11}	3.21×10^{13}
Low V_{disp}	14	18.88	0.888	55.9	5.54×10^{11}	2.75×10^{13}
Large L_X	11	24.11	1.411	90.3	5.54×10^{11}	7.06×10^{13}
Medium L_X	13	16.82	0.682	78.5	5.54×10^{11}	2.97×10^{13}
Low L_X	15	23.19	1.319	49.6	5.54×10^{11}	3.63×10^{13}

[a] N is the number of clusters in the subsample. The cutoffs for the $N_{0.5}$ subsamples were 10.2, 15.85, and 21.5 galaxies. The means were 6.9, 12.4, 18.4, and 26.9 galaxies. The cutoffs for the V_{disp} subsamples were 655, and 785 km s^{-1}. The means were 504, 720, and 945 km s^{-1}. The cutoffs for the L_X subsamples were 4.6, and 14.0 ergs cm^{-2} s^{-1}. The means were 2.30, 7.51, and 34.4 ergs cm^{-2} s^{-1}.

[b] $E\%_{2.0}$ is the elliptical percentage for the galaxies within 2.0 Mpc of the cluster centers.

[c] Δ is the enhancement of $E\%_{2.0}$ assuming an intrinsic value of 10% [i.e., $(E\%_{2.0} - 10)/10$].

[d] $N_{2.0}$ is the number of galaxies within 2.0 Mpc of the cluster centers. Corrections for foreground/background galaxies and the magnitude cutoff have been made.

[e] Constant is $1.54 \times L \times M/L$; where 1.54 is the correction factor for galaxies dimmer than -20.4, $L = 6 \times 10^{10}\ L_\odot$ is the luminosity of a typical galaxy, and 6 is the assumed mass-to-light ratio. See text for more details.

[f] $M_{\text{X-ray gas}}$ is the predicted value of the mass of the X-ray gas. It is determined by multiplying cols. (4), (5), and (6).

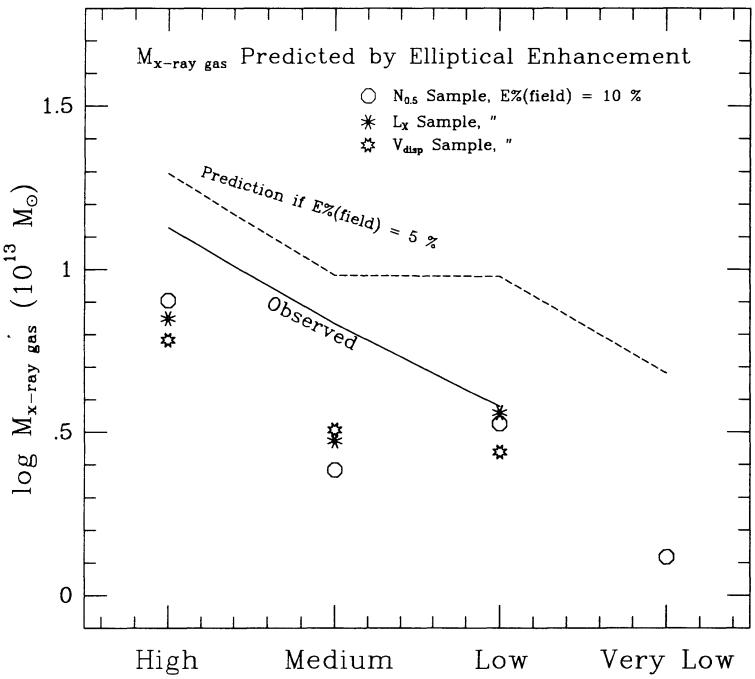

FIG. 14.—Mass of the X-ray gas as predicted by the enhancement of the elliptical fraction near the centers of the clusters (see text and Table 3 for details of the calculation). The data points show the values for the various subsamples of $N_{0.5}$, V_{disp}, and L_X. The solid line shows the observed values of $M_{X\text{-ray gas}}$ as a function of the L_X subsamples (Jones et al. 1993). The dashed line shows the average of the predicted values from the elliptical enhancement if a value of 5% is used for the intrinsic elliptical percentage.

some of the gas was primordial and was never associated with a protogalaxy. This would mean that our estimate should be lower than the observed value, the amount depending on how much X-ray gas was primordial. If about 40% of the gas in the intracluster medium was primordial and 60% was from failed spiral and S0 galaxies, the observations and predictions would match.

Another possibility is that some fraction of the elliptical galaxies may not have collapsed by the time the cluster collapsed and would therefore be destroyed along with the spiral and S0 galaxies. This would also result in an underestimate of the predicted value of $M_{X\text{-ray gas}}$.

Still another possible enhancement to the model would be to have the spiral and S0 bulges form at the same time as the ellipticals, and only allow the material from the slowly forming disk to be removed during the cluster collapse. This would not affect the model very much since the luminosity of the bulge is generally 2–3 mag dimmer than the disk, hence most of the mass would still be returned to the intergalactic medium. The leftover bulge components would generally be dimmer than the magnitude cutoff and hence would not be included in our number counts. This scenario might also explain why low-luminosity ellipticals are rapidly rotating like spiral bulges; they are just the relics of protospirals whose disks were never allowed to form.

While the general agreement between the model and the observations is reassuring, the simplicity of the model warrants caution in making very specific conclusions at this time.

4.4.2. *Possible Mechanisms: the Mean Tidal Field of the Cluster*

It should be possible to determine whether tidal shear from the mean field of the cluster is a viable physical mechanism by calculating tidal radii and comparing them with the observed radii of different types of galaxies. For example, according to the model we should find that elliptical galaxies are smaller than their tidal radii throughout the cluster, since ellipticals are assumed to be indestructible. S0 and spiral galaxies that have already formed should also be smaller than their tidal radii, except perhaps in the inner few tenths of a Mpc where the observed fractions of these types of galaxies are nearly zero. However, the protogalaxies should be larger than the tidal radii over a wide range of the cluster and especially near the center. We will assume a protogalaxy was 10 times the size of a present-day galaxy, as suggested by Fall & Efstathiou (1980) based on angular momentum considerations.

The tidal radius for a galaxy can be approximated by the equation (Binney & Tremaine 1987).

$$r_{tidal} \approx [m_{galaxy}(r)/3M_{cluster}(R)]^{1/3}R\ ,$$

where r_{tidal} is the tidal radius of the galaxy, $m_{galaxy}(r)$ is the mass of the galaxy within a galactocentric radius of r, and $M_{cluster}(R)$ is the mass of the cluster within a clustercentric radius of R.

Figure 15 shows the tidal radii for a typical 5×10^{11} $M_\odot$ galaxy as a function of position in the cluster, and for cluster masses of 10^{14} and 10^{15} $M_\odot$ within the central 1.0 Mpc (solid lines). We assume that $M_{cluster} \propto R$. Tidal effects would be stronger for a more concentrated profile. Typical values of the current radii at the twenty-fifth B isophote are also included for the different morphological types (long-dashed lines). The intersection of the two lines represents the clustercentric radius at which tidal effects becomes important for already formed galaxies. The dotted line shows a more detailed model from Merritt (1984), which is in reasonable agreement with our simple model in the range 0.15–1.0 Mpc. The short-dashed lines show the radii for protogalaxies, assuming a factor of 10 increase in radius from their current size.

We find that current ellipticals would be immune to the tidal field throughout essentially the entire cluster. Only within

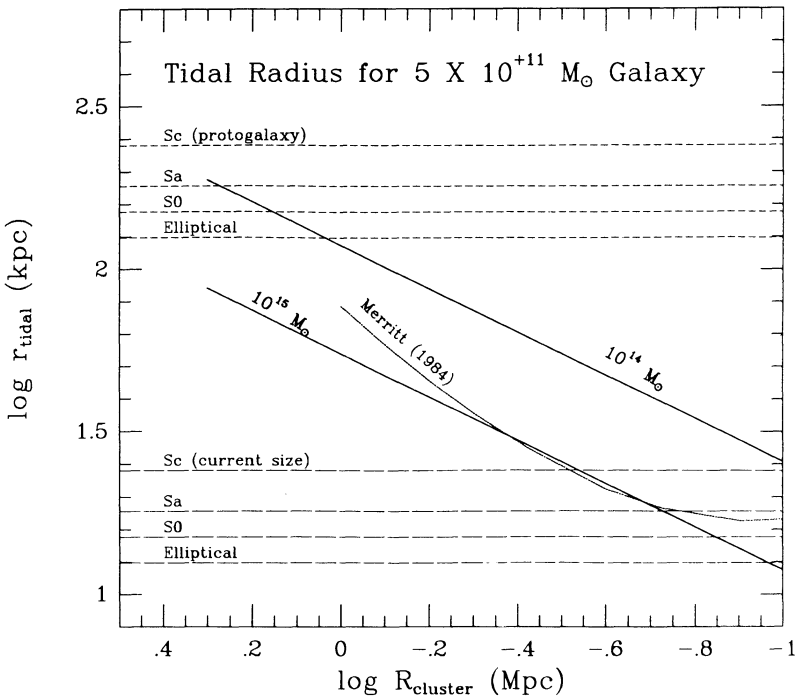

FIG. 15.—A rough estimate of the tidal radius as a function of $R_{\rm cluster}$ for cluster masses of 10^{14} and 10^{15} $M_\odot$ within 1 Mpc of the cluster center, and a galaxy mass of 5×10^{11} $M_\odot$ (*solid lines*). Typical values of the radii for different types of galaxies are also indicated, both during the current epoch (*long-dashed lines*), and for the original protogalaxy (*short-dashed lines*). The intersection of the lines shows where tidal stripping becomes important. The dotted line shows the tidal radii from a more detailed model by Merritt (1984).

about 0.1 Mpc of the most massive cluster centers would ellipticals be affected. However, our simple assumptions about the cluster profile may break down in this region, as suggested by Merritt's (1984) more realistic model. On the other hand, S0 and spiral galaxies are affected farther out in the cluster, especially the Sc galaxies. For example, Figure 15 indicates that for a typical cluster with 10^{15} $M_\odot$, current Sc galaxies should be affected at about $R = 0.28$ Mpc, while current Sa galaxies would be affected at about $R = 0.18$ Mpc. This may explain the fact that the number of Sc galaxies is essentially zero out to about 0.4 Mpc in Figure 13, while the hole in the Sa galaxies is only out to about 0.1 Mpc. Protogalaxies are found to be affected much farther out in the cluster, as required by one of the assumptions in our model.

The effect of the tidal shear depends quite sensitively on the core radius of the mass profile. In fact, the primary reason Merritt (1984) found stronger tidal effects than earlier studies such as Malumuth & Richstone (1983) was the use of a smaller core radius (i.e., 125 h^{-1} kpc). Recent results based on gravitational lensing by clusters (Tyson 1991) indicate that even smaller values for the core radius are probably more reasonable (i.e., 50 h^{-1} kpc), hence the mean field of the cluster may have a stronger effect than even Merritt suggested.

4.4.3. *Possible Mechanisms: Galaxy-Galaxy Interactions*

Another potential mechanism that has been examined by several authors (e.g., Spitzer & Baade 1951; Richstone 1974; Larson et al. 1980; de Souza et al. 1982; Merritt 1984; Mamon 1986) is the effect of collisions between individual galaxies. Most of these studies have only modeled the global effects on the group or cluster, making it difficult to ascertain whether the rapid rise in the elliptical fraction within 0.5 Mpc of the cluster center can be reproduced. However, it is clear from these studies that a large fraction of the mass can be removed if the collision cross sections are on the order of 60 kpc or larger, as would clearly be the case for protogalaxies. Most of the damage occurs during the original cluster collapse, which limits the usefulness of making estimates based on current conditions in the clusters. This may also indicate that only the inner regions of clusters have collapsed, since that is the only region where large elliptical enhancements are observed. Several groups (e.g., Evrard 1992) are currently constructing detailed *n*-body simulations of clusters where each galaxy is represented by enough particles to begin to study the structure and dynamics of individual galaxies. This approach may provide definitive answers concerning which physical mechanisms are most relevant in clusters.

5. DISCUSSION

The issue of which is more fundamental, the morphology-density relation or the morphology-radius relation, is not just a semantic question. The goal is to identify the relevant physical mechanisms responsible for determining the morphological fractions in clusters. The fact that the morphology-radius relation appears to be the more fundamental correlation suggests that global mechanisms, rather than local mechanisms, are responsible for controlling the morphological fractions in clusters.

One of the surprising results of this study was finding that the morphological fractions appears to only depend on one parameter, the normalized cluster radius, $R/R_c^{\rm opt}$. A high percentage of ellipticals is found in the very center of nearly all clusters, even if they are very diffuse, have low velocity dispersions, or low X-ray luminosities. Spirals are almost completely absent in the centers of all clusters. These results would seem to

indicate that clusters are quite similar, at least the central regions of clusters. Perhaps it indicates that the cores of nearly all clusters have gone through a collapse phase.

Our original hope in this project was to learn something about how galaxies form. As it turns out, we have probably learned more about how galaxies are destroyed. The fact that rapid changes in the gradients are only seen near the cluster centers leads to a model where protogalactic clouds, which were destined to become spirals and S0s, are destroyed during the cluster collapse. The model assumes that material from the failed galaxies forms much of the intergalactic medium in clusters. This provides a link between the morphological fractions and the X-ray properties of the cluster. It also provides a quantitative tool for testing some of the evolutionary models suggested roughly a decade ago (Larson et al. 1980; Gunn 1982; Meisels & Ostriker 1984; Postman & Geller 1984; Merritt 1984).

While the model is quite simplistic in nature, and will almost certainly require important modifications (e.g., the inclusion of primordial X-ray gas that was never associated with a protogalaxy), the wide range of observations it is able to explain suggests that an understanding of the fate of protogalaxies in clusters may be the key to understanding the morphological fractions.

We would like to thank Alan Dressler for providing his computer files containing the measurements for the 55 clusters he studied. We continue to be amazed by both the quality and quantity of this data base. We would also like to thank Kirk Borne, Bill Forman, Bill Oegerle, Jerry Ostriker, Marc Postman, Craig Sarazin, Ian Whitmore, and Steve Zepf for useful discussions, and Carolyn Stern for help compiling some of the X-ray data.

REFERENCES

Amran, P., Sullivan, W. T., Balkowski, C., Marcelin, M., & Cayatte, C. 1992, preprint
Arnaud, M., Rothenflug, R., Boulade, O., Vigroux, L., & Vangioni-Flam, E. 1992, A&A, 254, 49
Babul, A., & Postman, M. 1990, ApJ, 359, 280
Bahcall, N. 1977, ApJ, 217, L77
Beers, T. C., & Tonry, J. L. 1986, ApJ, 300, 557
Bingelli, B., Tammann, G. A., & Sandage, A. 1987, AJ, 94, 251
Binney, J. 1980, in X-Ray Astronomy, ed. R. Giacconi & G. Setti (Boston: Reidel), 245
Binney, J., & Tremaine, S. 1987, in Galactic Dynamics (Princeton: Princeton Univ. Press), 450
Bower, R. G., Lucey, J. R., & Ellis, R. S. 1991, MNRAS, 254, 601
Charlton, J., Whitmore, B. C., & Gilmore, D. 1992, in Groups of Galaxies, ed. O. Richter (Provo: ASP Conf. Series), in press
David, L., Arnaud, K., Forman, W., & Jones, C. 1990, ApJ, 356, 32
David, L., Forman, W., & Jones, C. 1991, ApJ, 380, 39
de Souza, R. E. Capelato, H. V., Arakaki, L., & Logullo, C. 1982, ApJ, 263, 557
Distefano, A., Rampazzo, R., Chincarini, G., & de Souza, R. 1990, A&AS, 86, 7
Dressler, A. 1980, ApJ, 236, 351
———. 1984, ARA&A, 22, 185
———. 1986, ApJ, 301, 35
Dressler, A., & Shectman, S. A. 1988, AJ, 94, 899
Eggen, O. J., Lynden-Bell, D., & Sandage, A. 1962, ApJ, 136, 748
Evrard, A. E. 1992, in Physics of Nearby Galaxies: Nature or Nurture, ed. T. X. Thuan, C. Balkowski, & T. T. Van (Gif sur Yvette: Éditions Frontières), in press
Evrard, A. E., Silk, J., & Szalay, A. S. 1990, ApJ, 365, 66
Faber, S. M., & Gallagher, J. S. 1979, ARA&A, 17, 135
Fall, S. M., & Efstathiou, G. 1980, MNRAS, 193, 189
Fitchett, M. 1988, in The Minnesota Lectures on Clusters of Galaxies and Large-Scale Structure, ed. J. M. Dickey (San Francisco: Astron. Soc. Pacific), 143
Geller, M. J., & Huchra, J. P. 1983, ApJS, 52, 61
Giovanelli, R., Haynes, M. P., & Chincarini, G. L. 1986, ApJ, 300, 77
Gott, J. R., & Thuan, T. X. 1976, ApJ, 204, 649
Gunn, J. E. 1982, in Astrophysical Cosmology, ed. H. A. Bruck, G. V. Coyne, & M. S. Longair (Vatican City: Pontifica Academica Scientifica Scripta Varia), 233
Hatsukade, I. 1989, Ph.D. thesis, Osaka Univ.
Hickson, P., Kindl, E., & Huchra, J. P. 1988, ApJ, 331, 64
Hubble, E., & Humason, M. L. 1931, ApJ, 74, 43
Huchra, J. P., Geller, M. J., de Lapparent, V., & Corwin, H. G., Jr. 1990, ApJS, 72, 433
Jones, C., Hughes, J., Stern, C., & Forman, W. 1993, in preparation
Larson, R. B. 1990, PASP, 653, 704
Larson, R. B., Tinsley, B. M., & Caldwell, C. N. 1980, ApJ, 237, 692
Maia, M. A. O., & Da Costa, L. N. 1990, ApJ, 352, 457
Malumuth, E. M., & Richstone, D. O. 1983, ApJ, 268, 30
Mamon, G. A. 1986, ApJ, 307, 426
———. 1987, ApJ, 321, 622
Maoz, E. 1990, ApJ, 359, 257
Meisels, A., & Ostriker, J. P. 1984, AJ, 89, 1451
Melnick, J., & Sargent, W. L. W. 1977, ApJ, 215, 401
Merritt, D. 1984, ApJ, 276, 26
Oemler, A., Jr. 1974, ApJ, 194, 1
Postman, M., & Geller, M. J. 1984, ApJ, 281, 95
Richstone, D. O. 1974, ApJ, 204, 642
Rood, H. J., & Williams, B. A. 1989, ApJ, 339, 772
Sanromà M., & Salvador-Solé, E. 1990, ApJ, 360, 16
Schechter, P. L. 1976, ApJ, 203, 297
Shaya, E. J., & Tully, R. B. 1984, ApJ, 281, 56
Spitzer, L., & Baade, W. 1951, ApJ, 113, 413
Struble, M. F., & Rood, H. J. 1991, ApJS, 77, 363
Sulentic, J. A. 1987, ApJ, 322, 605
Tully, R. B., & Shaya, E. J. 1984, ApJ, 281, 31
Tyson, J. A. 1991, in Texas/ESO-CERN Symp. on Relativistic Astrophysics (New York: New York Academy of Science), 164
Whitmore, B. C. 1990, in Clusters of Galaxies, ed. W. Oegerle, L. Danly, & M. Fitchett (Cambridge: Cambridge Univ. Press)
———. 1991, in Galaxy Environments and the Large Scale Structure of the Universe, ed. G. Giuricin, F. Mardirossian, & M. Mezzetti (Trieste: SISA)
———. 1992, in Groups of Galaxies, ed. O. Richter (Provo: ASP Conf. Series), in press
Whitmore, B. C., Forbes, D. A., & Rubin, V. C. 1988, ApJ, 333. 542
Whitmore, B. C., & Gilmore, D. M. 1991, ApJ, 367, 64 (WG)
Wyse, R. F. G. 1985, ApJ, 299, 593